

AD/COM

~~X67-11487~~

~~92~~ ~~92~~

~~OR 80890~~ ~~07~~

FACILITY FORM 802

(NASA CR OR TMX OR AD NUMBER) (CATEGORY)

Final Report
Task V

SNR Behavior of Coherent Phase Demodulators
RADIO COMMUNICATIONS STUDY
ON NOISE THRESHOLD REDUCTION

30 September 1965

Contract NAS5-9742

Prepared by

ADCOM, Inc.
808 Memorial Drive
Cambridge, Massachusetts 02139

for

National Aeronautics and Space Administration
Goddard Space Flight Center
Greenbelt, Maryland

N68-14275

(ACCESSION NUMBER)

(THRU)

(CODE)

(CATEGORY)

(PAGES)

(NASA CR OR TMX OR AD NUMBER)

FACILITY FORM 802

Final Report
Task V

SNR Behavior of Coherent Phase Demodulators

RADIO COMMUNICATIONS STUDY
ON NOISE THRESHOLD REDUCTION

30 September 1965

Contract NAS5-9742

by

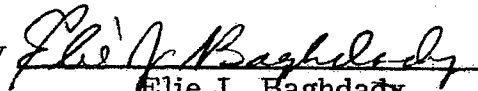
Ahmad F. Ghais

Richard H. Wachsman

Prepared by

ADCOM, Inc.
808 Memorial Drive
Cambridge, Massachusetts 02139

Approved by



Elie J. Baghdady
Technical Director

for



National Aeronautics and Space Administration
Goddard Space Flight Center
Greenbelt, Maryland

PRECEDING PAGE BLANK NOT FILMED.

ABSTRACT

An analysis of the signal-to-noise ratio at the outputs of three types of coherent phase detectors is performed for the case of sinusoidal phase modulation at various values of phase deviation and a perfectly coherent reference. The phase detectors studied are the conventional multiplier, the sinusoidal phase detector preceded by a limiter, and the cross-over detector. These phase detectors are frequently employed as phase demodulators in PM telemetry systems.

The output noise power is evaluated both in the absence and in the presence of modulation. The results are presented in the form of input-output SNR curves. In the case of noise measured in the absence of modulation, good agreement between theoretical and experimental results is achieved. The output noise measured in the presence of modulation is found to include modulation distortion components and modulation/noise interaction components.

A threshold effect is found to occur for the sinusoidal phase detector preceded by a limiter and the cross-over detector, but not for the conventional multiplier. The SNR degradation below threshold is not as catastrophic as that for wideband FM. This fact makes PM in conjunction with coherent phase demodulation more attractive at low input SNR than FM. It was also found that the conventional multiplier gave the best performance at low input SNR.

TABLE OF CONTENTS

Section		Page
I.	INTRODUCTION.	1
	1.1 Purpose of the Report	1
	1.2 Scope of the Report	1
II.	INTERPRETATION OF THE MEASUREMENTS	5
	2.1 Description of the SNR Measurements	5
	2.2 Description of Analytical Approach	5
	2.3 The Conventional Multiplier	7
	2.4 Cross-over Detector.	9
	2.5 Discussion and Recommended Alternate Measurements.	16
III.	ANALYSIS OF SNR BEHAVIOR.	21
	3.1 SNR Behavior of a Phase Detector Preceded by a Limiter	21
	3.1.1 Output Signal Power for a Sinusoidal Modulating Signal.	22
	3.1.2 Output Noise Power for a Sinusoidal Modulating Signal.	25
	3.2 Sinusoidal Phase Detector Preceded by a Limiter	26
	3.2.1 Calculation of S_o	27
	3.2.2 Calculation of N_o	28
	3.3 Cross-over Detector.	34
	3.3.1 Calculation of S_o	34
	3.3.2 Calculation of N_o	38
	3.4 Conventional Multiplier as a Phase Detector	44
	3.5 Comparison of the SNR Behavior of the Three Phase Detectors	50
IV.	CONCLUSIONS	57
V.	PROGRAM FOR NEXT INTERVAL	61

TABLE OF CONTENTS (Cont.)

Section	Page
REFERENCES	63
APPENDIX A.	65
APPENDIX B.	75

LIST OF ILLUSTRATIONS

Figure		Page
1	Experimental test setup	6
2a	Conventional demodulation, $\beta_s = 1$ rad.	10
2b	Conventional demodulation, $\beta_s = 2$ rads	11
3	$T(\phi_e)$ for cross-over phase detector	12
4a	Cross-over detector (signal-to-noise ratio = 0.1, 1, 10 and ∞) from Chadima	14
4b	Cross-over detector (signal-to-noise ratio = 0.001, 0.01, 0.1 and ∞) from Chadima	15
5a	Cross-over detector, $\beta_s = 1$ rad.	17
5b	Cross-over detector, $\beta_s = 2$ rads	18
6	Functional block diagram of a phase detector preceded by a limiter	21
7	$\alpha^2(\rho) \sin$ and $(1 - \alpha^2(\rho) \sin)$	29
8	$\sigma_o^2(\rho) = \frac{1 - e^{-\rho}}{2\rho}$	30
9	SNR curves for sinusoidal phase detector preceded by a limiter.	33
10	Cross-over phase detector transfer function	35
11	Approximation of $m_1(\beta, \rho)$ obtained by truncating sum at $n = 2, 4, 6, 8, \infty$ for $\rho = 1.0$	37
12	$\frac{1}{2} (\alpha_o(\rho) \beta_s + \alpha_1(\rho) 2J_1(\beta_s))^2$ and $\epsilon(\beta_s, \rho)$	39
13	Square of the cross-over phase detector transfer function	40
14	$\sigma_{\theta_n}^2(\rho)$ and $\gamma(\beta_s, \rho)$	42
15	SNR curves for cross-over phase detector	45
16	SNR curves for the conventional multiplier.	48
17	Comparison of the SNR curves of the three phase detectors for $\beta_s = 0.5$ rad.	51
18	Comparison of the SNR curves of the three phase detectors for $\beta_s = 1.0$ rad.	52
19	Comparison of the SNR curves of the three phase detectors for $\beta_s = 1.5$ rads	53
20	Comparison of the SNR curves of the three phase detectors for $\beta_s = 2.0$ rads	54

LIST OF NOTATION

- ω_m - frequency of the sinusoidal modulating signal.
- β_s - peak phase deviation of the carrier phase by the sinusoidal modulating signal: $\beta(t) = \beta_s \sin \omega_m t$.
- ρ - signal-to-noise power ratio at the limiter input, $\rho = E_s^2 / 2\sigma_N^2$.
- E_s - the amplitude of the phase modulated IF carrier at the input to the limiter.
- σ_N^2 - the variance of $N_c(t)$ or $N_q(t)$, equal to the total input noise power.
- $N_c(t), N_q(t)$ - the cophasal and quadrature components of the noise at the input to the limiter. $N_c(t), N_q(t)$ are assumed to have gaussian probability density functions.
- $\beta(t)$ - phase modulation on the carrier.
- $m_1(\beta, \rho)$ - average output of the phase detector for fixed β and carrier-to-noise power ratio ρ .
- θ_n - the noise contribution to the total phase of the combined phase modulated carrier plus noise at the input to the phase detector.
- $q(\theta_n)$ - probability density function of θ_n .
- $\phi_i(t)$ - phase of the combined phase modulated carrier plus noise at the input to the limiter, $= \beta(t) + \theta_n(t)$.
- ϕ_r - phase of the reference carrier, assumed properly-phased and jitter-free so that $\phi_r = 0$.
- ϕ_e - instantaneous phase error into the phase detector, equal to the phase of the input phase modulated carrier plus noise minus the phase of the reference carrier, $= \phi_i - \phi_r$.
- $T(\phi_e)$ - the transfer function of the phase detector preceded by a limiter.

LIST OF NOTATION (Cont.)

- ω_{IF} - the IF carrier frequency.
- ϕ_{spe} - static phase error in the carrier-tracking phase-locked loop from which the reference is obtained.
- $\phi_j(t)$ - jitter on the reference carrier.
- $J_n(\beta_s)$ - Bessel function of the first kind of index n .
($n = 0, 1, 2, \dots$)
- S_o - signal power out of the phase detector at ω_m , measured in the presence of input noise.
- N_o - noise power out of the phase detector.
- $(S/N)_o$ - signal-to-noise power ratio out of the phase detector.
- $\text{erf}(x)$ - the error function.
- $$\text{erf}(x) = \frac{2}{\sqrt{\pi}} \int_0^x e^{-y^2} dy$$
- $\langle \rangle_t$ - time average
- $\psi(\tau)$ - auto-correlation function of the output of the phase detector preceded by a limiter.
- $\psi_p(\tau)$ - the auto-correlation function of the periodic component of the output of the phase detector preceded by a limiter, equal to the periodic part of $\psi(\tau)$ when $\beta = \beta_s \sin \omega_m t$.
- $p_{\beta, \theta_n}(\beta_1, \beta_2, \theta_{n_1}, \theta_{n_2})$ - joint probability density function of $\beta(t_1)$, $\beta(t_2 = t_1 + \tau)$, $\theta_n(t_1)$, and $\theta_n(t_2 = t_1 + \tau)$.
- $p_{\beta}(\beta_1, \beta_2)$ - joint probability density function of $\beta(t_1)$, $\beta(t_2 = t_1 + \tau)$.
- $q_{\beta}(\beta)$ - probability density function of β .
- $A_k(\beta_s, \rho)$ - amplitude of the k^{th} Fourier harmonic of $m_1(\beta_s \sin \omega_m t, \rho)$.
- $m_2(\beta, \rho)$ - the total output power of the phase detector for fixed β and input signal-to-noise power ratio ρ .

LIST OF NOTATION (Cont.)

$\alpha(\rho)_{\sin}$	- signal suppression factor for the sinusoidal phase detector preceded by a limiter.
$\sigma_o^2(\rho)$	- noise power out of the sinusoidal phase detector preceded by a limiter in the absence of modulation.
${}_1F_1\left(\frac{3}{2}, 2; \rho\right)$	- confluent hypergeometric function.
$\alpha_o(\rho)$	- coefficient of the β term in the $m_1(\beta, \rho)$ function for the cross-over detector.
$\alpha_1(\rho)$	- coefficient of the $\sin\beta$ term in the $m_1(\beta, \rho)$ function for the cross-over detector.
$\alpha_n(\rho)$	- coefficient of the $I_n(\beta)$ term in the $m_1(\beta, \rho)$ function for the cross-over detector.
$I_n(\beta)$	- a function of β which appears in the calculation of $m_1(\beta, \rho)$ for the cross-over detector.
$G_n(\rho)$	- a function of ρ which appears in the calculation of $m_1(\beta, \rho)$ for the cross-over detector.
$F_n(\beta_s)$	- a function of β_s appearing in the calculation of $A_1(\beta_s, \rho)$ for the cross-over detector.
$\epsilon(\beta_s, \rho)$	- that part of $S_o(\beta_s, \rho)$ for the cross-over detector which involves the functions $F_n(\beta_s)$.
$\sigma_{\theta_n}^2(\rho)$	- the variance of θ_n , equal to the noise power out of the cross-over detector in the absence of modulation.
$H_n(\beta)$	- a function of β appearing in the calculation of $m_2(\beta, \rho)$ for the cross-over detector.
$E_n(\beta_s)$	- a function of β_s appearing in the calculation of $\langle m_2(\beta_s \sin \omega_m t, \rho) \rangle_t$ for the cross-over detector.
$\gamma(\beta_s, \rho)$	- that part of $N_o(\beta_s, \rho)$ for the cross-over detector which depends on β_s .
A	- the amplitude (normalized to E_s) of the combined signal plus noise at the input to the limiter.
$p_j(A, \theta_n)$	- joint probability density function of A and θ_n .
$b_{n,k}$	- a coefficient in the expansion of $(1 - \cos \phi)^n$ in terms of the functions $\cos k\phi$.

I. INTRODUCTION

1.1 Purpose of the Report

This report comprises the fourth final task report on the results of a program of investigations carried out at ADCOM, Inc. under Contract No. NAS 5-9742 for NASA. This work was conducted in close coordination with, and in direct support of activities of members of the RF Systems Branch, Advanced Development Division of the Goddard Space Flight Center.

The effort during the quarter 1 June 1965 - 31 August 1965 was allocated exclusively to performing the fifth task of the study program. Since the task was completed in one quarter, no quarterly reports are contractually required for the fourth quarter.

1.2 Scope of the Report

The objective of the fifth task of the subject contract is to investigate demodulation techniques to permit receiver operation with a minimum of SNR deterioration. In particular, we concentrate our attention in this report on:

- a. The SNR deterioration in the cross-over phase detector, and
- b. The SNR deterioration in the conventional phase detector (with or without a limiter).

The ultimate objective of the joint NASA-ADCOM effort is to attain a complete understanding of the noise performance of coherent phase detectors, and to evaluate possible schemes for improving their performance.

The SNR behavior of coherent phase detectors employed in telemetry receivers is examined in Section II. Both the multiplier type and cross-over (sawtooth) phase detectors are considered, under conditions of sinusoidal modulation and additive narrowband gaussian noise. The signal power at the output of the phase detector is considered to be that measured by a narrowband ac voltmeter tuned to the frequency of the sinusoidal modulation; whereas the noise power is considered to be that measured by a true power meter placed at the

output of the phase detector, but with the modulation turned off. We predict analytically the behavior of these measurements, compare the predictions with the measurements made by members of the RF Systems Branch, identify the primary causes of SNR degradation, and, in the light of these results, propose further SNR measurements which serve to characterize the phase detectors more fully.

We point out in Section II that a better characterization of the SNR behavior of phase detectors would be obtained if the output noise power were to be measured in the presence of modulation. In order to accomplish this, the true power meter which measures the output noise power must be preceded by a notch filter tuned to the modulation frequency. The noise power measurement will then include the distortion harmonics of the signal and additional noise power which would disappear if the modulation was removed. We also point out that a third type of phase detector, namely the sinusoidal detector preceded by a limiter, should be examined since it is frequently employed in operational telemetry systems.

The purpose of Section III is to theoretically predict and compare the SNR behavior of the three commonly used phase detectors, namely:

- the conventional multiplier,
- the multiplier preceded by a limiter, and
- the cross-over detector.

The output noise is considered to be measured in the presence of modulation. The results are presented in the form of curves of the signal-to-noise power ratio out of the detector plotted as a function of input signal-to-noise power ratio, ρ , for several values of phase deviation β_s .

In Sec. 3.1 the general case of a phase detector preceded by a limiter is discussed for the case of a sinusoidal phase modulating signal, and a general

procedure for calculating the signal and noise powers out of the phase detector is evolved. The special cases of the sinusoidal phase detector preceded by a limiter and the cross-over detector are discussed in Secs. 3. 2 and 3. 3 respectively. The conventional multiplier as a phase detector is then discussed in Sec. 3. 4. The results for the three cases are compared in Sec. 3. 5. Finally, conclusions are drawn and some application considerations are presented in Section IV.

The results of this task were presented orally to the technical staff of the RF Systems Branch on two occasions:

<u>Date of Presentation</u>	<u>ADCOM Staff Participating</u>
5 August 1965	Ahmad F. Ghais Richard H. Wachsman
9 September 1965	Ahmad F. Ghais Richard H. Wachsman

In addition, most of the contents of this report were presented in the form of informal technical memoranda to the technical representative of the contracting officer, as follows:

<u>Tech. Memo. No.</u>	<u>Date</u>	<u>Title</u>
G-63-8	20 August 1965	SNR Behavior of Phase Detectors.
G-63-9	30 September 1965	SNR Behavior of Coherent Phase Detectors, Part II.

A technical paper based on the results of this investigation was submitted for publication in the proceedings of the National Telemetry Conference to be held in Boston in May 1966. The paper is entitled "The SNR Characterization of Coherent Phase Detectors," and is authored by Ahmad F. Ghais and Richard H. Wachsman.

II. INTERPRETATION OF THE MEASUREMENTS

2.1 Description of the SNR Measurements

A block diagram of the experimental test setup is shown in Fig. 1. The sinusoidal modulating signal of frequency $\omega_m = 1$ kc phase modulates a carrier with an adjustable peak phase deviation, β_s . The input signal-to-noise power ratio, ρ , is varied by attenuating the output of the phase-modulated-carrier signal generator prior to amplification by an AGC-controlled telemetry receiver of noise bandwidth 300 kc.

The IF output of the telemetry receiver is fed into both the cross-over detector (linear sawtooth phase detector preceded by a limiter) and a conventional multiplier. The signal powers at the outputs of the phase detectors are measured by an rms meter after filtering at 1 kc by a narrowband (3 cps bandwidth) tuned amplifier. Noise powers are measured by an rms meter at the output of the phase detectors, but with the modulation turned off. SNR measurements are made over a range of input signal-to-noise power ratios from -25 db to +20 db, and for peak phase deviations of 1 and 2 radians. The reference carrier for each phase detector is obtained from a carrier-tracking phase-locked loop (noise bandwidth ≈ 30 cps) which incorporates the phase detector in question as part of the loop. The effects of jitter on the reference carrier, and of carrier-tracking static phase errors must therefore be considered at low input signal-to-noise power ratios where they are most noticeable. However, the analyses in this report are restricted to a properly phased and jitter-free reference carrier.

2.2 Description of Analytical Approach

In this section, the analysis is confined to interpreting the measurements performed by V. DiLosa of NASA GSFC. Theoretical analyses of a more complete characterization of the noise properties of phase detectors, including the sinusoidal phase detector preceded by a limiter, appear in Section III of this report.

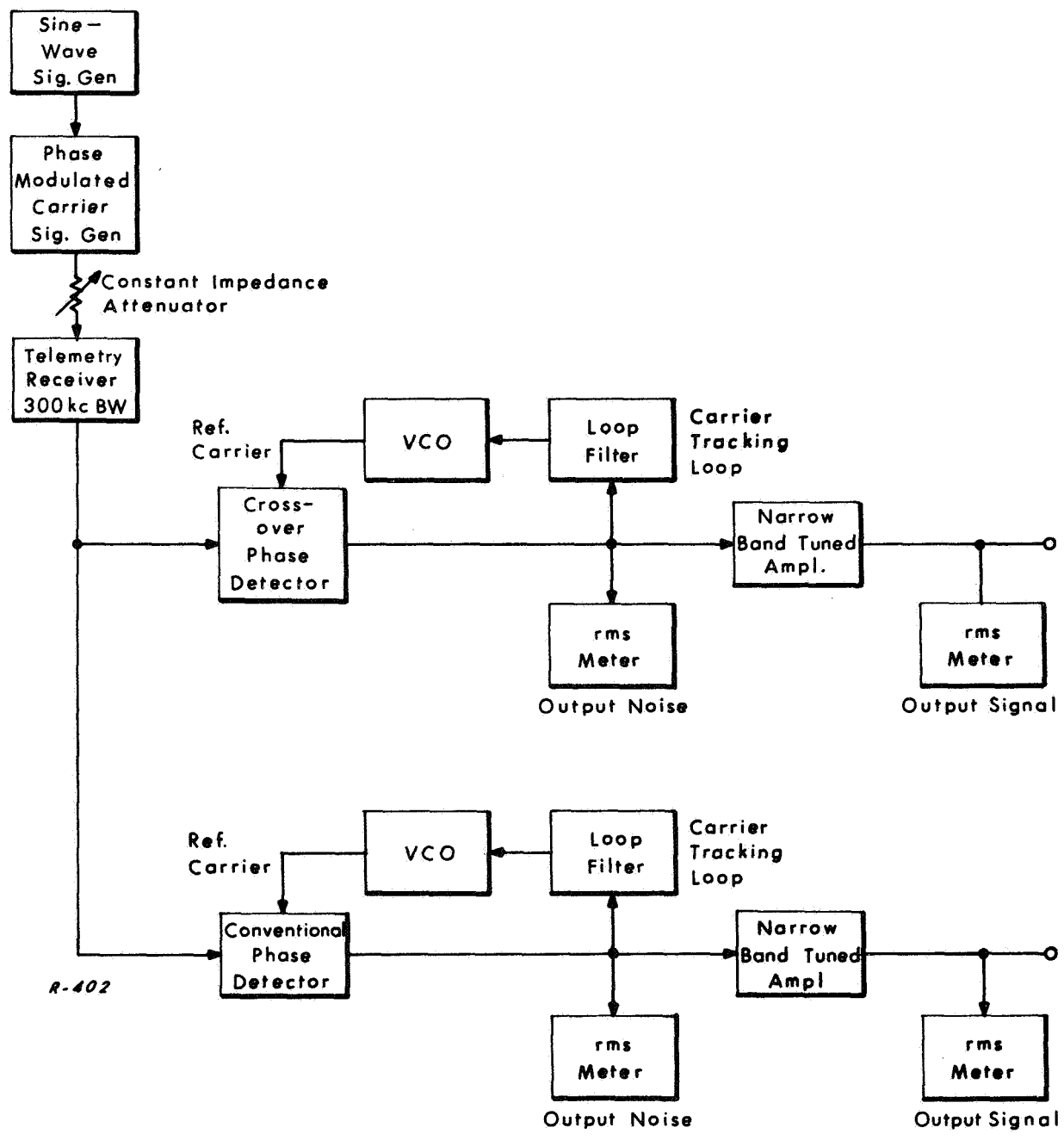


Fig. 1 Experimental test setup.

In Sec. 2.3, the conventional multiplier is discussed and SNR curves are calculated and compared with experiment.

In Sec. 2.4, the cross-over detector is analyzed by an extension of the work performed by Chadima.¹ Assuming a constant signal phase, β , the average value of the output of the cross-over detector, $m_1(\beta, \rho)$ is calculated as a function of β and the signal-to-noise power ratio, ρ . Knowledge of $m_1(\beta, \rho)$ enables us to calculate the output signal power in the presence of modulation. The variance of the output of the cross-over detector is also calculated. With $\beta = 0$, this is just the noise power that was measured.

These calculations are carried out by utilizing the nonlinear phase transfer function $T(\beta + \theta_n)$, and averaging over the noise component, θ_n , of the total phase, using the probability density function, $q(\theta_n)$. This is the appropriate procedure for a phase detector preceded by a limiter.

The effects of sinusoidal modulation are then taken into account, and the appropriate signal-to-noise ratio calculations performed in the limiting cases of $\rho \rightarrow \infty$ and $\rho \rightarrow 0$. The theoretical results are then compared with the experimental curves.

Section 2.5 is devoted to a discussion of the analytical approach and recommendation of alternate measurements.

2.3 The Conventional Multiplier

A conventional multiplier multiplies the input signal plus noise by the reference carrier, then lowpass filters the output, removing all double-carrier-frequency components. The noise at the input to the detector is assumed to be additive narrowband gaussian noise. The input signal plus noise may be written as

$$E_s \sin[\omega_{if}t + \beta(t)] + N_c(t) \sin[\omega_{if}t] + N_q(t) \cos[\omega_{if}t] \quad (1)$$

The reference carrier may be written in general as

$$\cos[\omega_{if} t + \phi_{spe} + \phi_j(t)] \quad (2)$$

where ϕ_{spe} is the static phase error representing imperfect phasing of the reference, and $\phi_j(t)$ is low frequency jitter.

The output of the detector may be represented, in normalized form, by

$$\begin{aligned} \sin[\beta(t) - \phi_{spe} - \phi_j(t)] - \frac{N_c(t)}{E_s} \sin[\phi_{spe} + \phi_j(t)] \\ + \frac{N_q(t)}{E_s} \cos[\phi_{spe} + \phi_j(t)] \end{aligned} \quad (3)$$

Since we are not considering the effects of non-zero ϕ_{spe} and $\phi_j(t)$ in this report, Eq. (3) may be written as

$$\sin[\beta(t)] + \frac{N_q(t)}{E_s} \quad (4)$$

With $\beta(t) = \beta_s \sin \omega_m t$, the signal component at ω_m becomes

$$e_s(t) = 2J_1(\beta_s) \sin \omega_m t \quad (5)$$

The total noise in the absence of modulation is just

$$e_N(t) = \frac{N_q(t)}{E_s} \quad (6)$$

The signal power is therefore

$$S_o = 2J_1^2(\beta_s) \quad (7)$$

and the noise power is simply

$$N_o = \frac{\langle N_q^2(t) \rangle_t}{E_s^2} = \frac{\sigma_N^2}{2\left(\frac{1}{2} E_s^2\right)} = \frac{1}{2\rho} \quad (8)$$

so that the output signal-to-noise ratio is given by

$$(S/N)_o = 4J_1^2(\beta_s) \rho \quad (9)$$

This is shown plotted for $\beta_s = 1$ rad. in Fig. 2a, and for $\beta_s = 2$ rads. in Fig. 2b. The experimental curves are also presented in these figures. There is strong reason to believe that the deviation of the experimental curves from linearity at small ρ is a result of improper phasing and jitter on the reference carrier.

2.4 Cross-over Detector

The total phase error, ϕ_e , may be written

$$\phi_e = \beta + \theta_n - \phi_{spe} - \phi_j \quad (10)$$

Again, since we are not considering the effects of non-zero ϕ_{spe} and $\phi_j(t)$ here, ϕ_e reduces to

$$\phi_e = \beta + \theta_n \quad (11)$$

The first order probability density function of θ_n is known to be given by¹

$$q(\theta_n) = \frac{e^{-\rho}}{2\pi} + \frac{1}{2} \sqrt{\frac{\rho}{\pi}} \cos \theta_n e^{-\{\rho \sin^2 \theta_n\}} \\ \times [1 + \operatorname{erf}(\sqrt{\rho} \cos \theta_n)] \quad -\pi \leq \theta_n \leq \pi \quad (12)$$

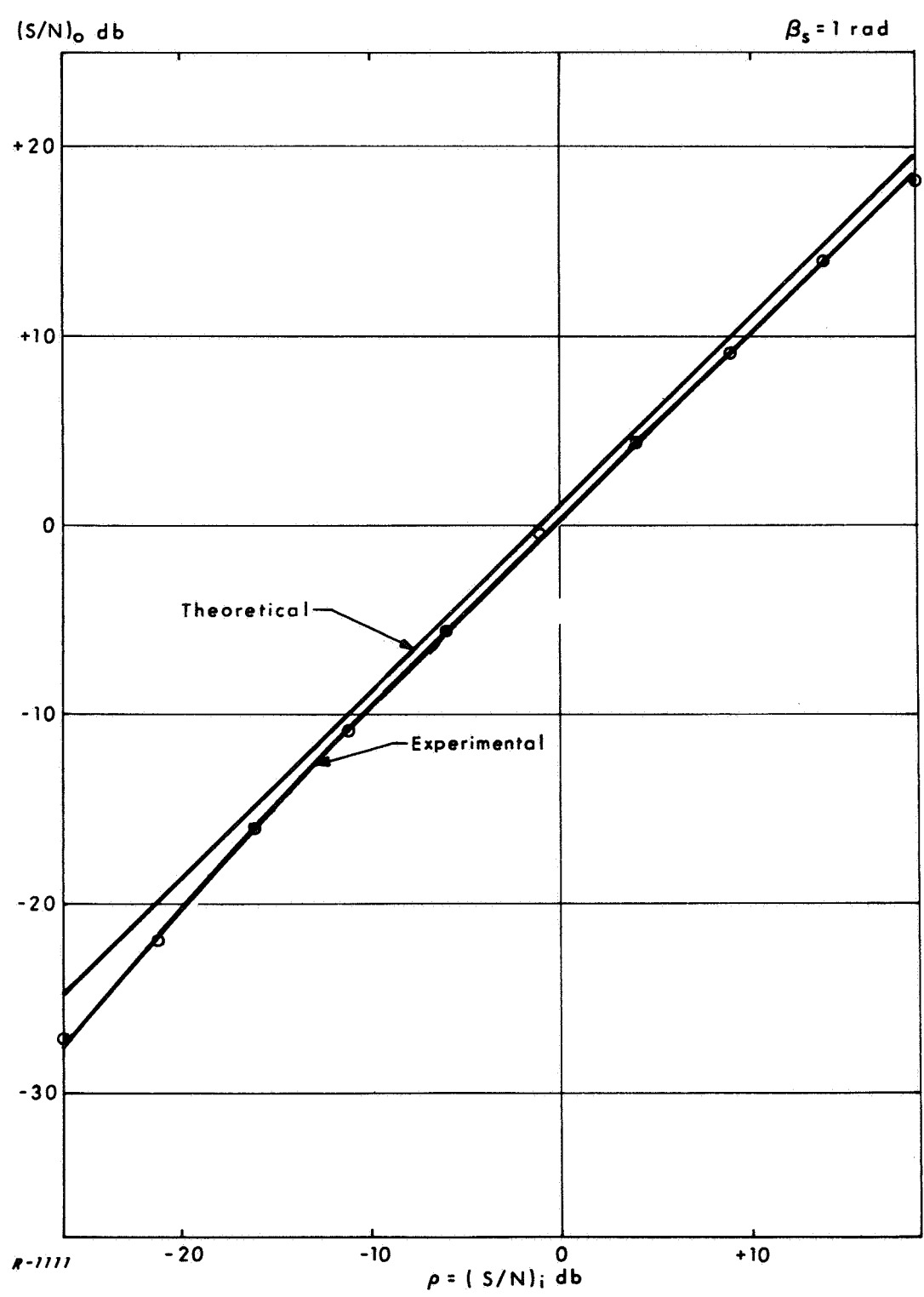


Fig. 2a Conventional demodulation, $\beta_s = 1$ rad.

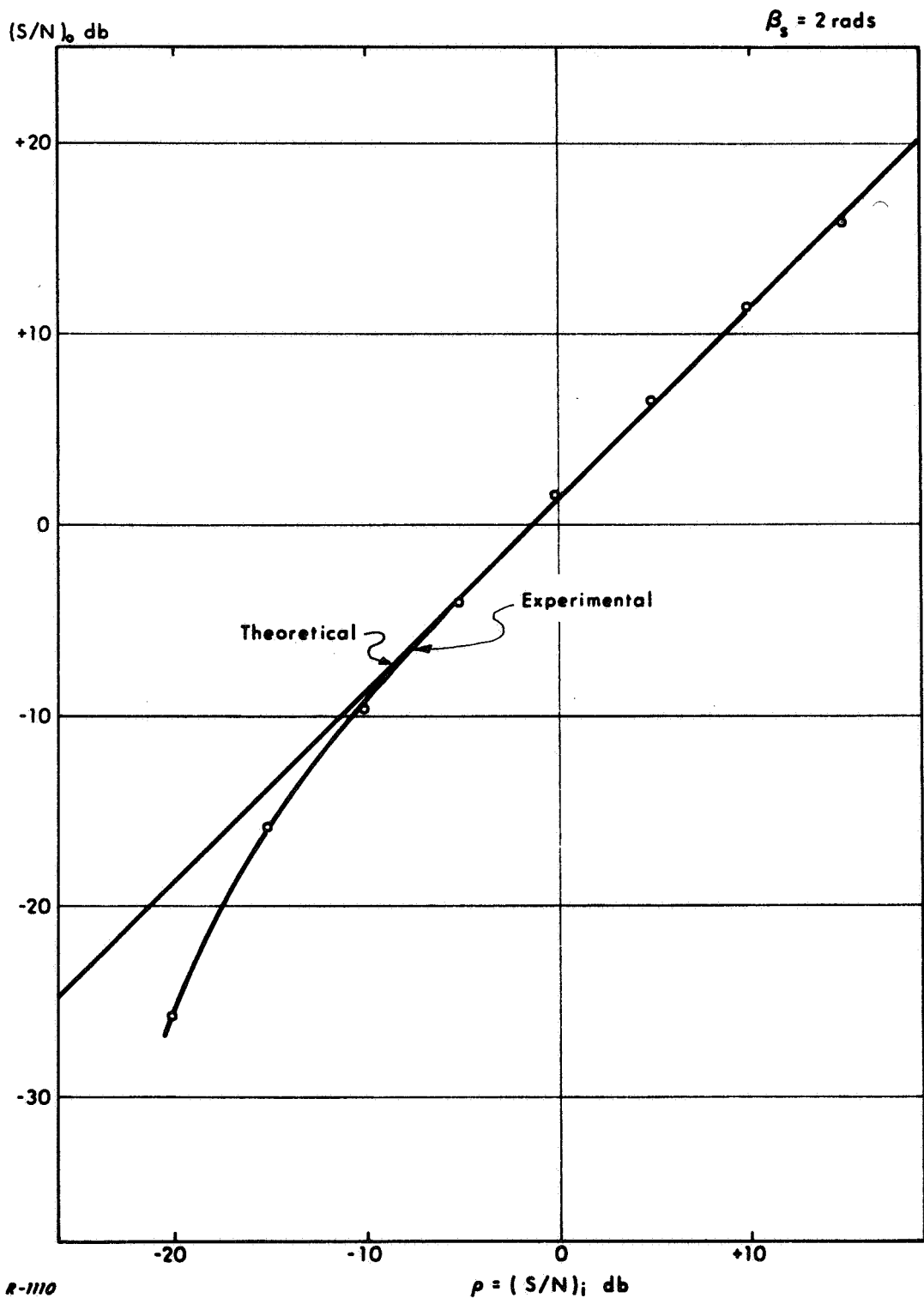


Fig. 2b Conventional demodulation, $\beta_s = 2$ rads.

where $\rho = E_s^2 / 2\sigma_N^2$ is the input signal-to-noise power ratio.

Let $T(\phi_e)$ represent the instantaneous transfer function of the phase detector. Then, for the cross-over detector

$$T(\phi_e) = \phi_e - 2n\pi \quad n = 0, \pm 1, \pm 2$$

$$(2n-1)\pi \leq \phi_e \leq (2n+1)\pi \quad (13)$$

This is plotted in Fig. 3.

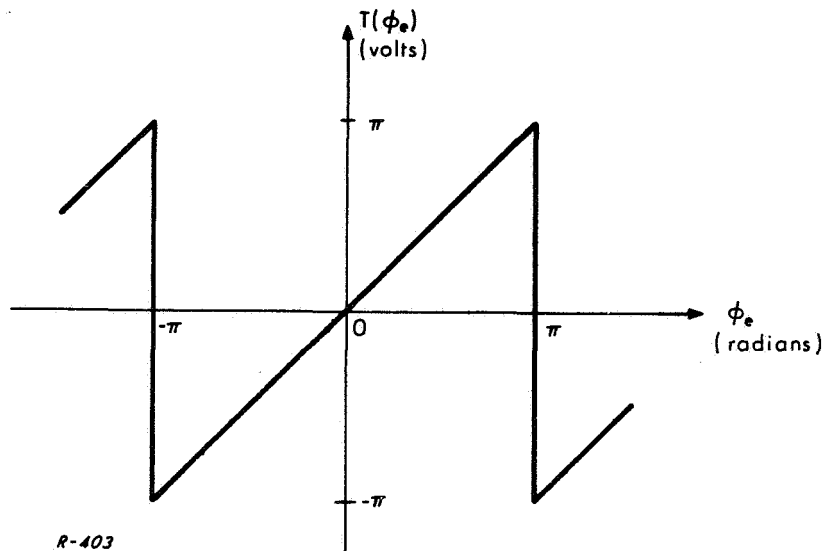


Fig. 3 $T(\phi_e)$ for cross-over phase detector.

Following Chadima¹, the average value of the output of the phase detector for a fixed value of β is calculated as a function of β and ρ . The average value is defined as

$$m_1(\beta, \rho) = \int_{-\pi}^{\pi} T(\beta + \theta_n) q(\theta_n) d\theta_n$$

$$m_1(\beta, \rho) = \begin{cases} \beta - 2\pi \int_{\pi-\beta}^{\pi} q(\theta_n) d\theta_n & \pi > \beta \geq 0 \\ \beta + 2\pi \int_{\pi-|\beta|}^{\pi} q(\theta_n) d\theta_n & -\pi < \beta \leq 0 \end{cases} \quad (14)$$

The integral

$$P(\pi - \beta < \theta_n < \pi) = \int_{\pi - \beta}^{\pi} q(\theta_n) d\theta_n \quad (15)$$

is difficult to evaluate in general, but may readily be evaluated in the strong and weak signal limits. An evaluation of this integral as an infinite series of functions of β , valid for all ρ , is presented in Appendix A.

In the weak signal limit, $m_1(\beta, \rho)$ approaches

$$m_1(\beta, \rho) (\rho \rightarrow 0) \rightarrow \sqrt{\pi\rho} \sin\beta \quad (16)$$

whereas, in the strong signal limit $m_1(\beta, \rho)$ approaches

$$m_1(\beta, \rho) (\rho \rightarrow \infty) \rightarrow \beta \quad -\pi < \beta < +\pi \quad (17)$$

Plots of $m_1(\beta, \rho)$ are shown in Figs. 4a and 4b. With $\beta = \beta_s \sin\omega_m t$, the component at ω_m in the output of the cross-over detector in these two limits is

$$e_s(t) (\rho \rightarrow 0) \rightarrow \sqrt{\pi\rho} 2J_1(\beta_s) \sin\omega_m t \quad (18)$$

$$e_s(t) (\rho \rightarrow \infty) \rightarrow \beta_s \sin\omega_m t \quad (19)$$

so that the signal powers become

$$S_o(\rho \rightarrow 0) \rightarrow 2\pi\rho J_1^2(\beta_s) \quad (20)$$

$$S_o(\rho \rightarrow \infty) \rightarrow \frac{1}{2} \beta_s^2 \quad (21)$$

The noise power is measured with modulation turned off ($\beta = 0$) and is given by

$$N_o = \int_{-\pi}^{\pi} \theta_n^2 q(\theta_n) d\theta_n = \sigma_{\theta_n}^2 \quad (22)$$

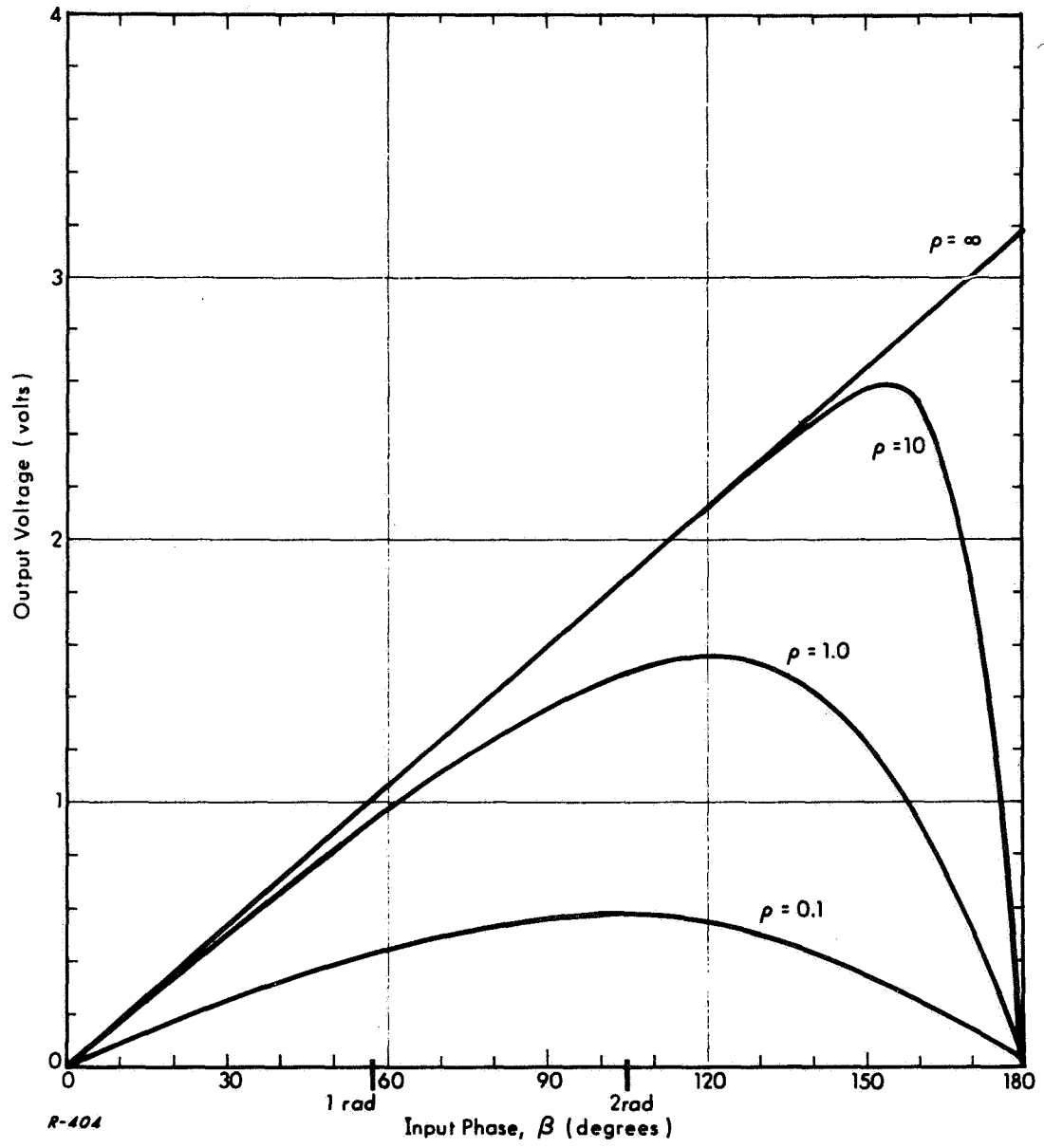


Fig. 4a Cross-over detector (signal-to-noise ratio = 0.1, 1, 10 and ∞) from Chadima.

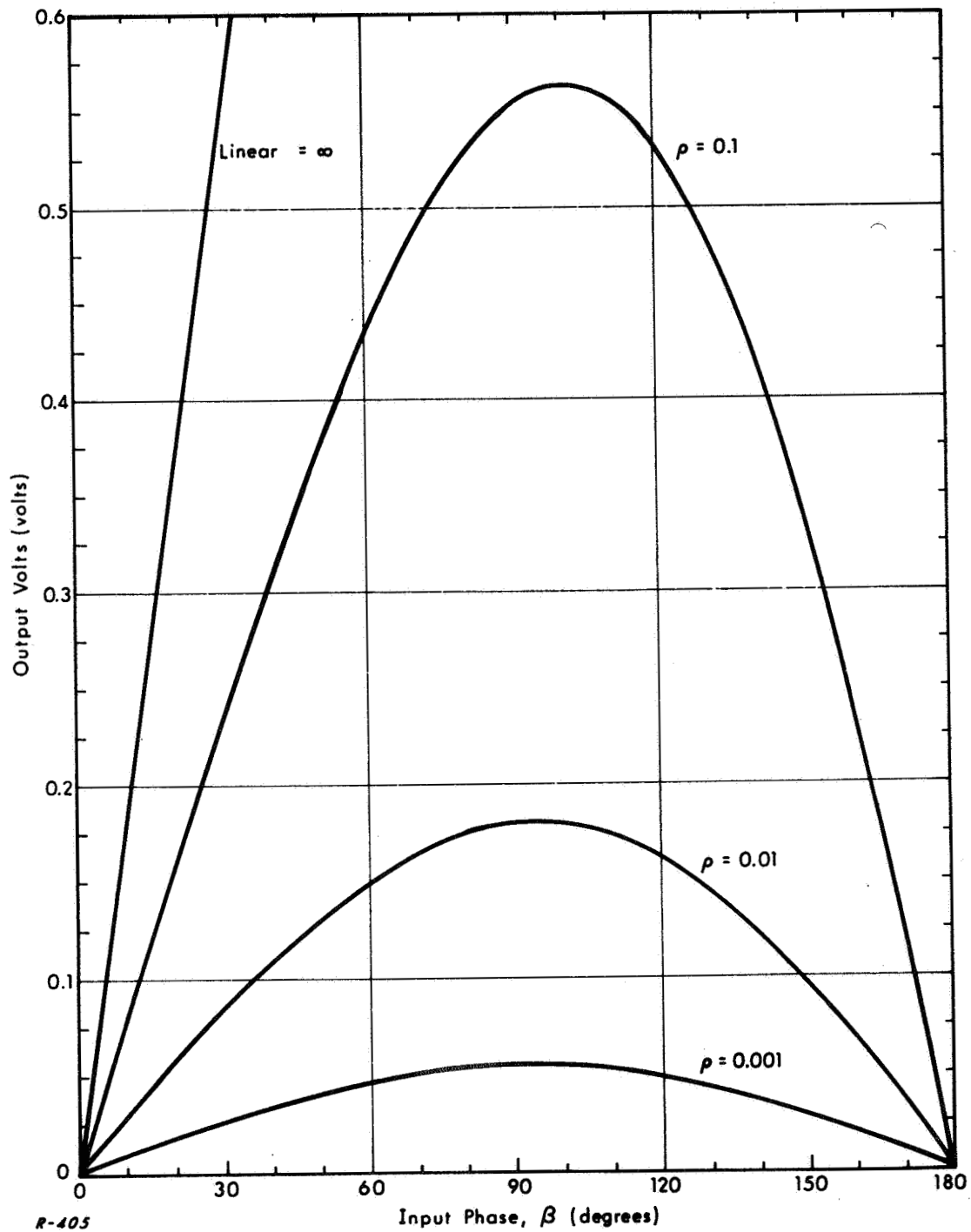


Fig. 4b Cross-over detector (signal-to-noise ratio = 0.001, 0.01, 0.1 and ∞) from Chadima.

In the weak and strong signal limits, the noise power becomes

$$N_o(\rho \rightarrow 0) \rightarrow \pi \frac{2}{3} \quad (23)$$

$$N_o(\rho \rightarrow \infty) \rightarrow \frac{1}{2} \rho \quad (24)$$

Hence the asymptotes of the SNR curves are

$$(S/N)_o(\rho \rightarrow 0) \rightarrow \frac{6}{\pi} J_1^2(\beta_s) \rho \quad (25)$$

and

$$(S/N)_o(\rho \rightarrow \infty) \rightarrow \beta_s^2 \rho \quad (26)$$

These asymptotes are plotted in Figs. 5a and 5b ($\beta_s = 1$ and 2 radians) along with the experimental results. Here again, the deviation of the experimental results from linearity as $\rho \rightarrow 0$ may be attributed to the effects of jitter and improper phasing of the reference.

2.5 Discussion and Recommended Alternate Measurements

In predicting the SNR behavior of the cross-over detector theoretically, the following approach was taken:

- a. The phase of the combined phase-modulated carrier plus noise was separated into the signal phase, $\beta(t)$, plus the noise contribution, θ_n , and the probability density distribution of θ_n was identified. (See Ref. 1).
- b. The phase error, ϕ_e , into the phase detector, was written as

$$\phi_e = \beta + \theta_n - \phi_{spe} - \phi_j(t).$$

- c. The reference carrier was assumed to be properly phased ($\phi_{spe} = 0$) and jitter free ($\phi_j(t) = 0$).

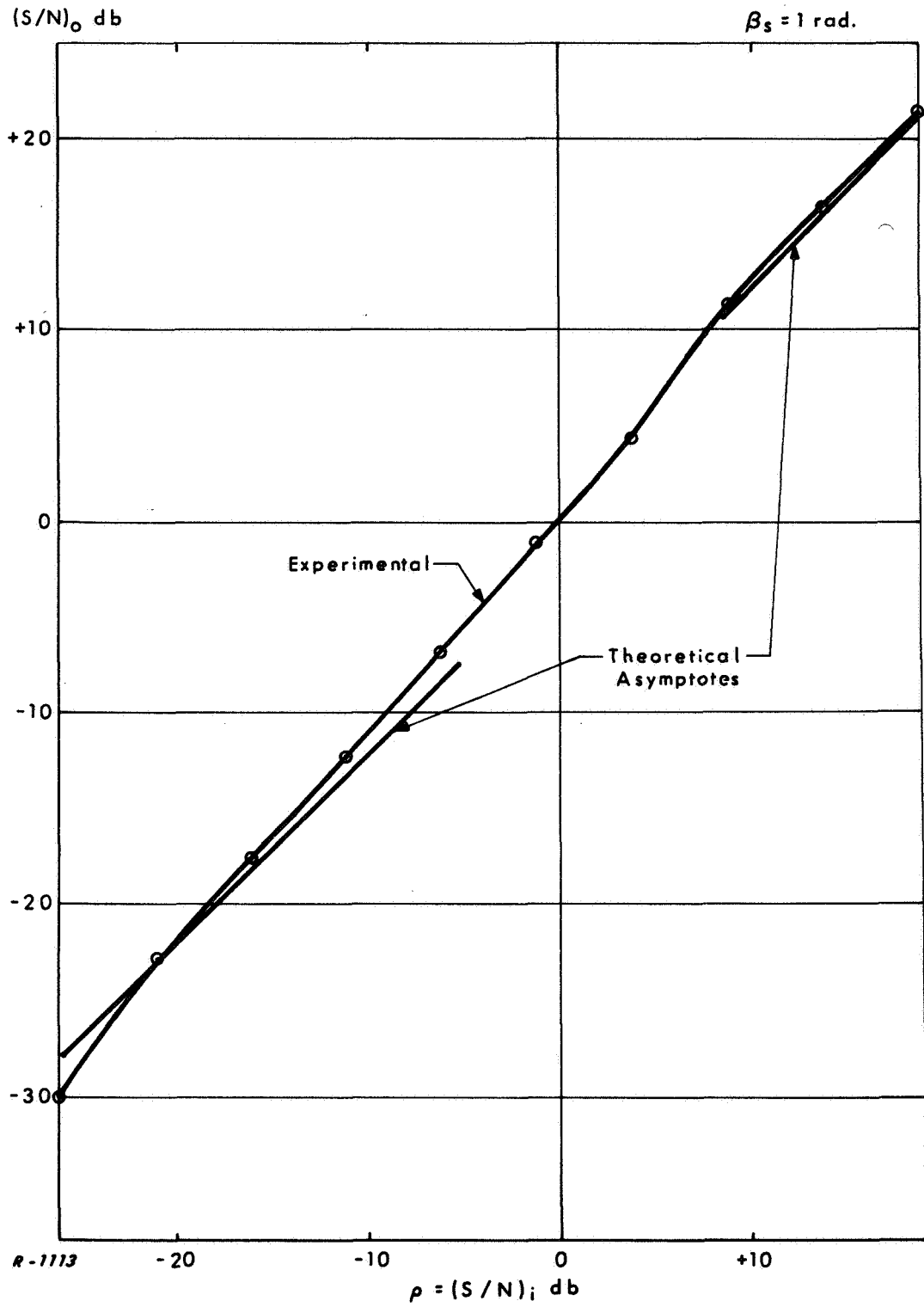


Fig. 5a Cross-over detector, $\beta_s = 1 \text{ rad.}$

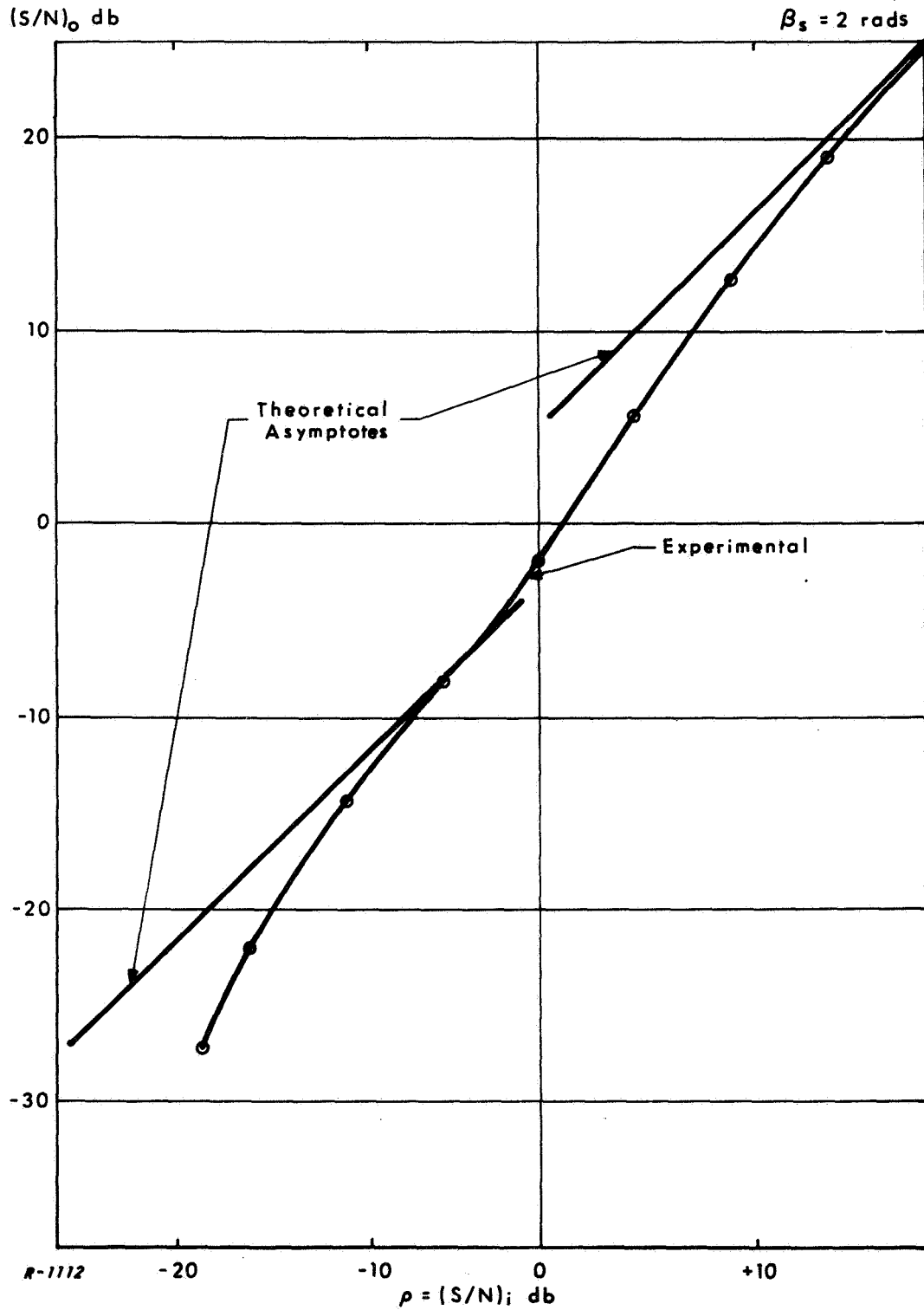


Fig. 5b Cross-over detector, $\beta_s = 2$ rads.

- d. The mean value of the phase detector output, $m_1(\beta, \rho)$, for a fixed β and ρ , was calculated by averaging $T(\beta + \theta_n(\rho))$ over θ_n .
- e. The resulting function $m_1(\beta, \rho)$ was plotted vs $\beta(0 < \beta < \pi)$ for fixed values of ρ . This function was seen to approach $T(\beta)$ as $\rho \rightarrow \infty$, and $\alpha(\rho) \sin \beta$ as $\rho \rightarrow 0$.
- f. The effect of modulation $\beta(t) = \beta_s \sin \omega_m t$ was taken into account by calculating the fundamental harmonic of $m_1(\beta_s \sin \omega_m t, \rho)$. This was done in the two limiting situations of $\rho \rightarrow \infty$ and $\rho \rightarrow 0$ where simple results may readily be obtained.
- g. The signal power, S_o , at ω_m was calculated in the asymptotic limits $\rho \rightarrow \infty$ and $\rho \rightarrow 0$.
- h. The noise power, $N_o = \sigma \theta_n^2$ was calculated (see Ref. 1) and the ratio $(S/N)_o$ formed for the asymptotic limits $\rho \rightarrow \infty$ and $\rho \rightarrow 0$.
- i. These theoretical results were compared with the experimental curves for $\beta_s = 1$ and 2 radians and agreement was generally found to be good with the exception that the experimental curve departed from linearity below -20 db for $\beta_s = 2$ rads. This is attributed to imperfect phasing and jitter on the reference carrier at such low input SNR.

SNR calculations were also made for the conventional multiplier, and the results compared with the experimental curves. Agreement was found to be good. The curves had the same slope and there was no SNR degradation below $\rho = +10$ db as in the case of the cross-over detector. Degradation caused by improper phasing and jitter on the reference carrier appeared in the experimental curves for this detector also, and at about the same values of ρ as in the cross-over detector.

In the light of these results the following experimental modifications are suggested:

- a. Phasing of the reference be checked and the IF frequency adjusted to equal the VCO free-running frequency as closely as possible.

- b. The noise bandwidth of the carrier-tracking loops be reduced from 30 cps by a factor of 5 or more.
- c. The bandwidth at the output of the phase detectors be at least 1 Mc, and the noise power measuring rms meter frequency response be flat to at least 1 Mc. This is necessary because the noise spectrum out of the phase detector is wider than the noise spectrum (limited by the amplifier bandwidth) into the detector.
- d. An alternate set of measurements be made with the noise power measured with the modulation on, and with a notch filter used to remove the signal component at 1 kc. The noise will therefore include the distortion harmonics of the signal and additional noise power present when $\beta \neq 0$.
- e. A complete set of measurements be made for a sinusoidal phase detector preceded by a limiter.

III. ANALYSIS OF SNR BEHAVIOR

3.1 SNR Behavior of a Phase Detector Preceded by a Limiter

The general problem of a phase detector preceded by a limiter is conveniently handled by studying the effect of the limiter and phase detector separately. The input to the limiter is considered to be a phase-modulated carrier plus additive, narrowband, gaussian noise. The output of the limiter is a waveform whose informational content is the instantaneous phase of the combined input signal plus noise. The instantaneous output of the phase detector, in general, is a single-valued nonlinear function of the difference between this phase and the phase of a reference carrier. This is indicated by the block diagram in Fig. 6.

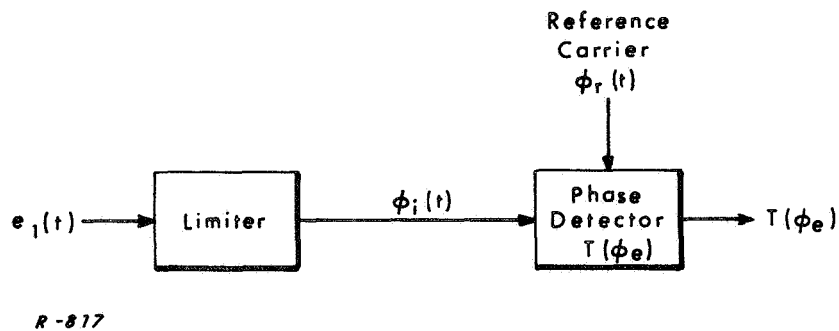


Fig. 6 Functional block diagram of a phase detector preceded by a limiter.

In mathematical terms, the output of the phase detector is $T(\phi_e = \phi_i - \phi_r)$, where $\phi_i(t)$ is the sum of the phase modulation of the carrier, $\theta_n(t)$, and a phase noise component, $\theta_n(t)$, $\phi_r(t)$ is the phase of a reference carrier, and $T(\phi_e)$ is the phase detector transfer function relating the phase detector output voltage to the phase difference $\phi_e = \phi_i - \phi_r$.

3.1.1 Output Signal Power for a Sinusoidal Modulating Signal

Measurements of the SNR behavior of phase detectors are commonly performed using a sinusoidal modulating signal

$$\beta(t) = \beta_s \sin \omega_m t \quad (27)$$

The signal power is measured at the output of a narrowband filter of center frequency ω_m placed at the output of the phase detector. The noise power is measured at the output of a narrowband notch filter of center frequency ω_m placed at the output of the phase detector. SNR data are usually presented in the form of a family of curves of the ratio of the signal-to-noise powers at the output of the phase detector plotted against the ratio of the power in the phase-modulated signal, $E_s^2/2$, to the noise power, σ_N^2 , at the input to the limiter, with the phase deviation β_s held constant. We now show how the behavior of these curves may be predicted theoretically.

We begin by writing the instantaneous phase detector output as

$$T[\beta_s \sin \omega_m t + \theta_n(t) - \phi_r(t)] \quad (28)$$

To proceed, we assume that the reference carrier is properly phased and jitter-free so that $\phi_r(t) = 0$. This is a valid assumption over a wide range of input signal-to-noise power ratios for the case where the reference is obtained from a carrier-tracking phase-locked loop.

Since the signal power out is defined as the power in the fundamental frequency component of the periodic part of the phase detector output, we must determine the average amplitude of this component. A convenient way of doing this utilizes a property of the autocorrelation function of a waveform containing a periodic component. It can be shown (see Ref. 2, p. 235) that the autocorrelation function of the periodic component of a waveform is the periodic component of the autocorrelation function of the total waveform. If this periodic component can be determined from the periodic part of the autocorrelation function, its Fourier series expansion can be developed and the amplitude, and hence the power, of the fundamental harmonic can be calculated.

The autocorrelation function of the output of the phase detector is the time average

$$\psi(\tau) = \left\langle T(\beta_s \sin \omega_m t + \theta_n(t)) \cdot T(\beta_s \sin \omega_m (t+\tau) + \theta_n(t+\tau)) \right\rangle_t \quad (29)$$

The periodic component of $\psi(\tau)$, $\psi_p(\tau)$, is obtained by evaluating (29) at sufficiently large values of τ so that the noise is uncorrelated. Replacing the time average by the equivalent ensemble average, (29) becomes

$$\begin{aligned} \psi(\tau = \tau_2 - \tau_1) &= \int d\beta_1 \int d\beta_2 \left[\int d\theta_{n_1} \int d\theta_{n_2} T(\beta_1 + \theta_{n_1}) T(\beta_2 + \theta_{n_2}) \right. \\ &\quad \left. \times p_{\beta, \theta_n}(\beta_1, \beta_2, \theta_{n_1}, \theta_{n_2}) \right] \end{aligned} \quad (30)$$

where $p_{\beta, \theta_n}(\beta_1, \beta_2, \theta_{n_1}, \theta_{n_2})$ is the joint probability density function of β_1 , β_2 , θ_{n_1} , and θ_{n_2} .

Since β and θ_n are assumed statistically independent, and since we are considering large τ so that θ_{n_1} and θ_{n_2} are also statistically independent,

$p_{\beta, \theta_n}(\beta_1, \beta_2, \theta_{n1}, \theta_{n2})$ may be factored as

$$p_{\beta, \theta_n}(\beta_1, \beta_2, \theta_{n1}, \theta_{n2}) = p_{\beta}(\beta_1, \beta_2) q(\theta_{n1}) q(\theta_{n2}) \quad (31)$$

where $p_{\beta}(\beta_1, \beta_2)$ is the joint probability density function of β_1 and β_2 , and $q(\theta_n)$ is the probability density function of θ_n obtained from the vector noise model (See Chadima¹). Accordingly, the periodic part of the autocorrelation function is obtained by combining (30) and (31) and integrating over θ_{n1} and θ_{n2} :

$$\psi_p(\tau = \tau_2 - \tau_1) = \int d\beta_1 \int d\beta_2 m_1(\beta_1, \rho) m_1(\beta_2, \rho) p_{\beta}(\beta_1, \beta_2) \quad (32)$$

where $m_1(\beta, \rho)$ is the first moment defined by

$$m_1(\beta, \rho) = \int_{-\pi}^{\pi} T(\beta + \theta_n) q(\theta_n) d\theta_n \quad (33)$$

The integration is carried out over the range $-\pi$ to $+\pi$ because both $T(\beta + \theta_n)$ and $q(\theta_n)$ are periodic with period 2π , and $q(\theta_n)$ is normalized so that

$$\int_{-\pi}^{\pi} q(\theta_n) d\theta_n = 1 \quad (34)$$

Now Eq. (32) may be converted to the equivalent time average

$$\psi_p(\tau) = \left\langle m_1(\beta_s \sin \omega_m t, \rho) \cdot m_1(\beta_s \sin \omega_m (t+\tau), \rho) \right\rangle_t \quad (35)$$

This is recognized as the autocorrelation function of the periodic function $m_1(\beta_s \sin \omega_m t, \rho)$, and hence we may identify this function as the periodic component of the output of the phase detector.

The periodic component $m_1(\beta_s \sin \omega_m t, \rho)$ may now be expanded into a Fourier series as

$$m_1(\beta_s \sin \omega_m t, \rho) = \sum_{k=0}^{\infty} A_k(\beta_s, \rho) \cdot \sin k \omega_m t \quad (36)$$

$$A_k(\beta_s, \rho) = 2 \left\langle m_1(\beta_s \sin \omega_m t, \rho) \cdot \sin k \omega_m t \right\rangle_t \quad (37)$$

The signal power at ω_m is therefore

$$S_o(\beta_s, \rho) = \frac{1}{2} A_1^2(\beta_s, \rho) = 2 \left\langle m_1(\beta_s \sin \omega_m t, \rho) \cdot \sin \omega_m t \right\rangle_t^2 \quad (38)$$

3.1.2 Output Noise Power for a Sinusoidal Modulating Signal

The noise power out of the phase detector is defined formally as the mean square of the difference between the total output of the phase detector and the fundamental frequency component at ω_m :

$$\begin{aligned} N_o(\beta_s, \rho) &= \left\langle \left[T(\beta_s \sin \omega_m t + \theta_n(t)) - A_1 \sin \omega_m t \right]^2 \right\rangle_t \\ &= \left\langle T^2(\beta_s \sin \omega_m t + \theta_n(t)) \right\rangle_t \end{aligned} \quad (39)$$

$$- 2A_1 \left\langle T(\beta_s \sin \omega_m t + \theta_n(t)) \cdot \sin \omega_m t \right\rangle_t + \frac{1}{2} A_1^2 \quad (40)$$

Converting the time averages of the first two terms of (40) to the equivalent ensemble averages in order to average over the noise, and then back to time averages in order to average over β , we obtain:

$$\left\langle T^2(\beta_s \sin \omega_m t + \theta_n(t)) \right\rangle_t = \int d\beta \int d\theta_n T^2(\beta + \theta_n) q(\theta_n) q_\beta(\beta) \quad (41)$$

$$= \int m_2(\beta, \rho) q_\beta(\beta) d\beta \quad (42)$$

$$= \left\langle m_2(\beta_s \sin \omega_m t, \rho) \right\rangle_t \quad (43)$$

where the second moment $m_2(\beta, \rho)$ is defined by

$$m_2(\beta, \rho) = \int_{-\pi}^{\pi} T^2(\beta + \theta_n) q(\theta_n) d\theta_n \quad (44)$$

The second term in (40) yields with the aid of (37)

$$\begin{aligned} & \langle T(\beta_s \sin \omega_m t + \theta_n(t)) \cdot \sin \omega_m t \rangle_t \\ &= \frac{1}{\beta_s} \int d\beta \int d\theta_n T(\beta + \theta_n) \beta q(\theta_n) q_\beta(\beta) \end{aligned} \quad (45)$$

$$= \frac{1}{\beta_s} \int \beta m_1(\beta, \rho) q_\beta(\beta) d\beta \quad (46)$$

$$= \langle m_1(\beta_s \sin \omega_m t, \rho) \cdot \sin \omega_m t \rangle_t \quad (47)$$

$$= \frac{1}{2} A_1(\beta_s, \rho) \quad (48)$$

Hence N_o becomes

$$N_o(\beta_s, \rho) = \langle m_2(\beta_s \sin \omega_m t, \rho) \rangle_t - \frac{1}{2} A_1^2(\beta_s, \rho) \quad (49)$$

This is recognized as the total power out of the phase detector minus the output signal power S_o .

The definition of the noise power given by (39) is more realistic than one which defines the noise power as the average power at the phase detector output with the modulation turned off. It remains to compute S_o and N_o from (38) and (49) for various types of phase detectors.

3.2 Sinusoidal Phase Detector Preceded by a Limiter

For the sinusoidal phase detector, $T(\phi_e)$ is given by

$$T(\phi_e) = \sin \phi_e \quad (50)$$

For $\phi_r = 0$ and $\beta = \beta_s \sin \omega_m t$, (24) becomes

$$T(\phi_i) = \sin [\beta_s \sin \omega_m t + \theta_n(t)] \quad (51)$$

We now employ Eqs. (38) and (49) to compute output signal and noise powers.

3.2.1 Calculation of S_o

In this case, $m_1(\beta, \rho)$ is given by

$$m_1(\beta, \rho) = \int_{-\pi}^{\pi} \sin(\beta + \theta_n) q(\theta_n) d\theta_n \quad (52)$$

Chadima¹ has shown that

$$m_1(\beta, \rho) = \alpha(\rho)_{\sin} \cdot \sin \beta \quad (53)$$

where the signal suppression factor $\alpha(\rho)_{\sin}$ is given by

$$\alpha(\rho)_{\sin} = \int_{-\pi}^{\pi} \cos \theta_n \cdot q(\theta_n) d\theta_n \quad (54)$$

$$= \sqrt{\frac{\pi\rho}{4}} e^{-\rho} {}_1F_1\left(\frac{3}{2}, 2; \rho\right) \quad (55)$$

${}_1F_1(3/2, 2; \rho)$ is a confluent hypergeometric function, a graph of which is available in Fig. 159 of Ref. 3.

We now expand the periodic component of the phase detector output in a Fourier series by making use of the relationship

$$\sin(\beta_s \sin \omega_m t) = 2 \sum_{\substack{n=1, 3, \dots \\ (n\text{-odd})}}^{\infty} J_n(\beta_s) \sin n\omega_m t \quad (56)$$

Hence $A_1(\beta_s, \rho)$ is

$$A_1(\beta_s, \rho) = \alpha(\rho)_{\sin} 2 J_1(\beta_s) \quad (57)$$

so that the signal power out, $S_o(\beta_s, \rho)$, is

$$S_o(\beta_s, \rho) = \frac{1}{2} A_1^2(\beta_s, \rho) = 2 J_1^2(\beta_s) \alpha^2(\rho)_{\sin} \quad (58)$$

The functions $\alpha^2(\rho)_{\sin}$ and $(1 - \alpha^2(\rho)_{\sin})$, a quantity which will be needed in the study of N_o , are plotted in Fig. 7.

3.2.2 Calculation of N_o

In this case, $m_2(\beta, \rho)$ is given by

$$m_2(\beta, \rho) = \int_{-\pi}^{\pi} \sin^2(\beta + \theta_n) q(\theta_n) d\theta_n \quad (59)$$

Trigonometric manipulation yields

$$m_2(\beta, \rho) = \sin^2 \beta + (\cos^2 \beta - \sin^2 \beta) \int_{-\pi}^{\pi} \sin^2 \theta_n q(\theta_n) d\theta_n \quad (60)$$

$$= \frac{1}{2} (1 - \cos 2\beta) + \sigma_o^2(\rho) \cos 2\beta \quad (61)$$

The integral in (60), which represents the noise power out in the absence of modulation was shown by Chadima¹ to be

$$\sigma_o^2(\rho) = \int_{-\pi}^{\pi} \sin^2 \theta_n q(\theta_n) d\theta_n = \frac{1 - e^{-\rho}}{2\rho} \quad (62)$$

This is plotted in Fig. 8.

With $\beta = \beta_s \sin \omega_m t$, we have

$$\begin{aligned} \langle m_2(\beta_s \sin \omega_m t, \rho) \rangle_t &= \frac{1}{2} (1 - \langle \cos(2\beta_s \sin \omega_m t) \rangle_t) \\ &\quad + \langle \cos(2\beta_s \sin \omega_m t) \rangle_t \sigma_o^2(\rho) \end{aligned} \quad (63)$$

Since

$$\langle \cos(2\beta_s \sin \omega_m t) \rangle_t = J_o(2\beta_s) \quad (64)$$

Eq. (63) becomes

$$\langle m_2(\beta_s \sin \omega_m t, \rho) \rangle_t = \frac{1}{2} [1 - J_o(2\beta_s)] + J_o(2\beta_s) \sigma_o^2(\rho) \quad (65)$$

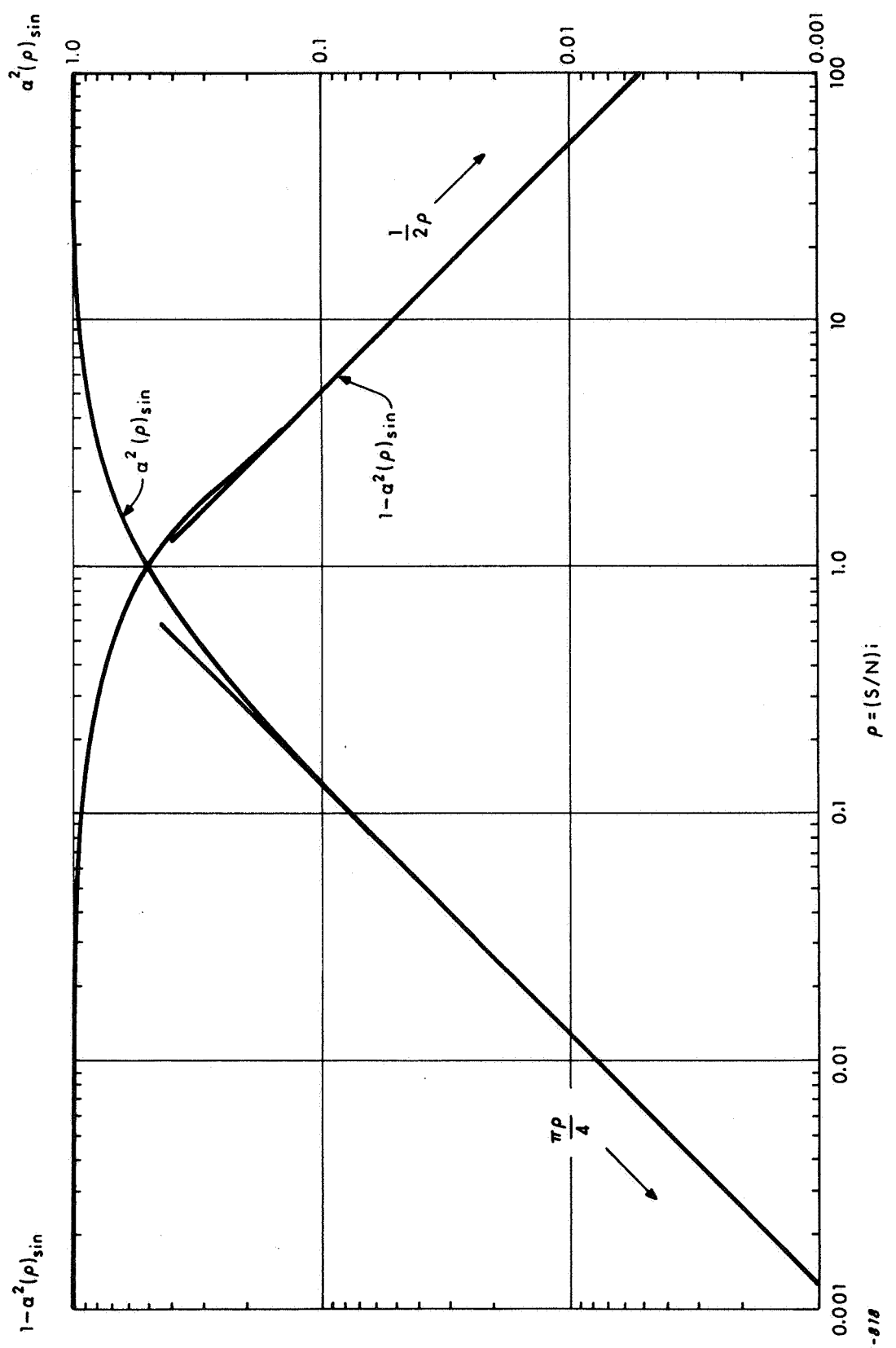


Fig. 7 $\alpha^2(\rho) \sin$ and $(1 - \alpha^2(\rho) \sin)$

R-818

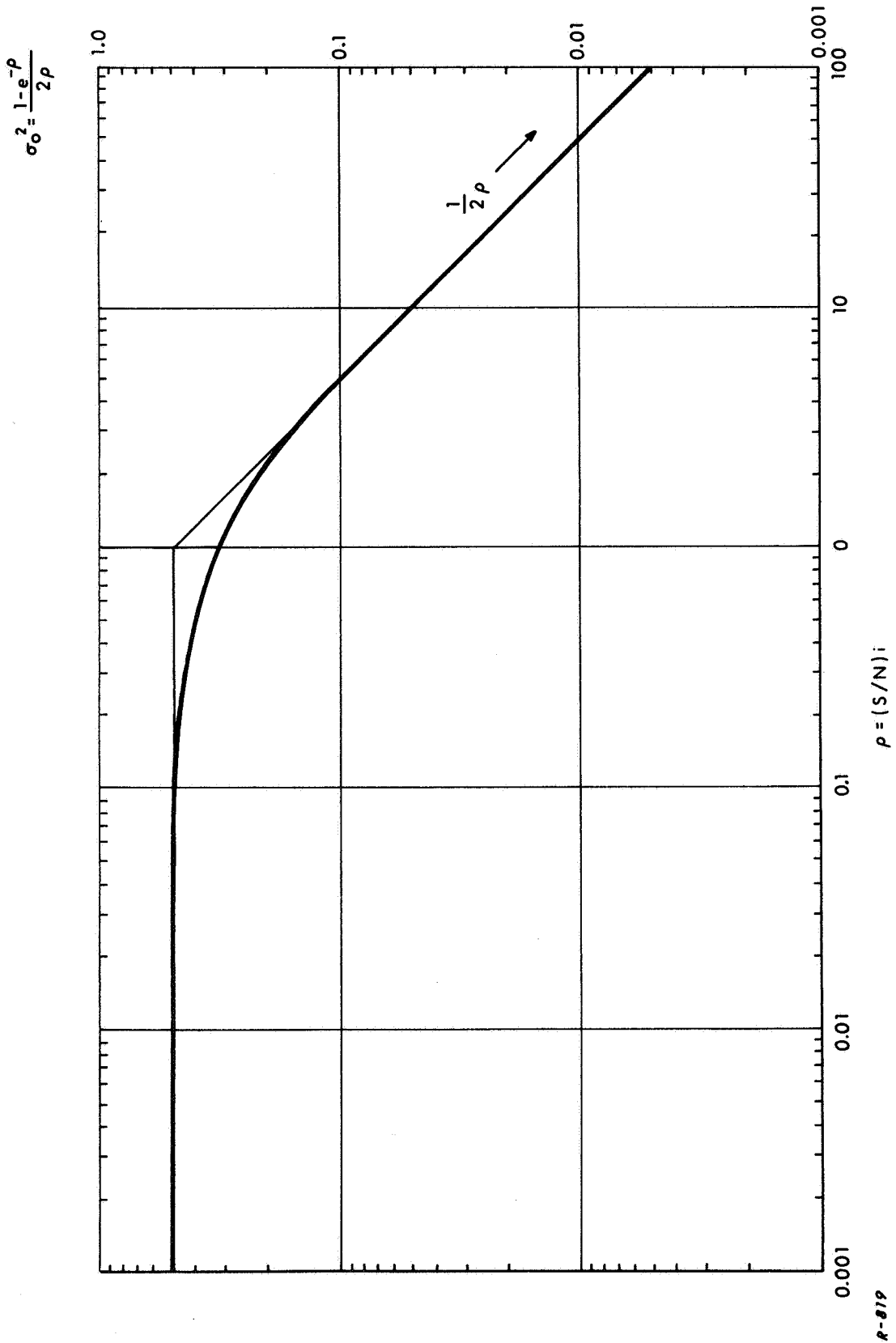


Fig. 8 $\sigma_o^2(\rho) = \frac{1-e^{-\rho}}{2\rho}$

R-819

Finally, the noise power N_o is obtained by combining (49), (58), and (65):

$$N_o(\beta_s, \rho) = \frac{1}{2} [1 - J_o(2\beta_s)] + J_o(2\beta_s) \sigma_o^2(\rho) - 2J_1^2(\beta_s) \alpha^2(\rho) \sin \quad (66)$$

An equivalent form of N_o , more useful at high SNR, utilizes the relationship

$$\frac{1}{2} [1 - J_o(2\beta_s)] = 2J_1^2(\beta_s) + 2 \sum_{\substack{n=3,5,\dots \\ (n-\text{odd})}}^{\infty} J_n^2(\beta_s) \quad (67)$$

and is

$$N_o(\beta_s, \rho) = J_o(2\beta_s) \sigma_o^2(\rho) + 2 \sum_{\substack{n=3,5,\dots \\ (n-\text{odd})}}^{\infty} J_n^2(\beta_s) + 2J_1^2(\beta_s) (1 - \alpha^2(\rho) \sin) \quad (68)$$

The various terms in (68) may be interpreted as follows. Since $\sigma_o^2(\rho)$ is the noise power in the absence of modulation, the first term represents a reduction in this power as a result of the presence of modulation. This reduction comes about because the maximum incremental gain, or slope, of the phase detector transfer function occurs at $\phi_e = 0$. With no modulation $\phi_e = \theta_n(t)$, and the noise jitter is always centered at the point of maximum incremental gain. When the modulation is turned on the noise jitter spends a large fraction of time centered at points of lower incremental gain, and hence the effect of modulation is to reduce the average contribution of the $\sigma_o^2(\rho)$ term to the total noise power.

The second term in (68) represents power in the higher order harmonics of ω_m resulting from the nonlinearity of the phase detector transfer function. The magnitude of this term depends only on β_s , and is independent of input signal-to-noise ratio ρ . It is this term which predominates at high input signal-to-noise ratios.

The third term in (68) is equal to the difference between the signal power at $\rho = \infty$ and $\rho = \rho$. This term may be thought of as an intermodulation between the signal and noise caused by the nonlinear phase detector transfer function. The result of this intermodulation is to cause a fraction $(1 - \alpha^2(\rho)_{\sin})$ of the power that, in the absence of noise, would lie at ω_m to become spread out over the frequency spectrum and hence add to the total noise power. The simplicity of (68) and the above interpretation is a result of the sinusoidal form of the phase detector transfer function; no comparable simplicity should be expected for other types of phase detectors.

The output signal-to-noise ratio is obtained by dividing (58) by (68)

$$(S/N)_o = \frac{2J_1^2(\beta_s) \alpha^2(\rho)_{\sin}}{J_0^2(2\beta_s) \sigma_o^2(\rho) + 2 \sum_{\substack{n=3,5,\dots \\ (n-\text{odd})}} J_n^2(\beta_s) + 2J_1^2(\beta_s)(1 - \alpha^2(\rho)_{\sin})} \quad (69)$$

This is plotted in Fig. 9 for $\beta_s = 0.5, 1.0, 1.5,$ and 2.0 radians.

The asymptotic behavior of $(S/N)_o$ at large and small ρ is

$$(S/N)_o (\rho \rightarrow \infty) \rightarrow \frac{J_1^2(\beta_s)}{\sum_{\substack{n=3,5,\dots \\ (n-\text{odd})}} J_n^2(\beta_s)} \quad (70)$$

and

$$(S/N)_o (\rho \rightarrow 0) \rightarrow \frac{J_1^2(\beta_s) \frac{\pi}{2} \rho}{\frac{1}{2} J_0^2(2\beta_s) + 2 \sum_{\substack{n=3,5,\dots \\ (n-\text{odd})}} J_n^2(\beta_s) + 2J_1^2(\beta_s)} \quad (71)$$

or, from the alternate form of N_o given in (66),

$$(S/N)_o (\rho \rightarrow 0) \rightarrow \pi \rho J_1^2(\beta_s) \quad (72)$$

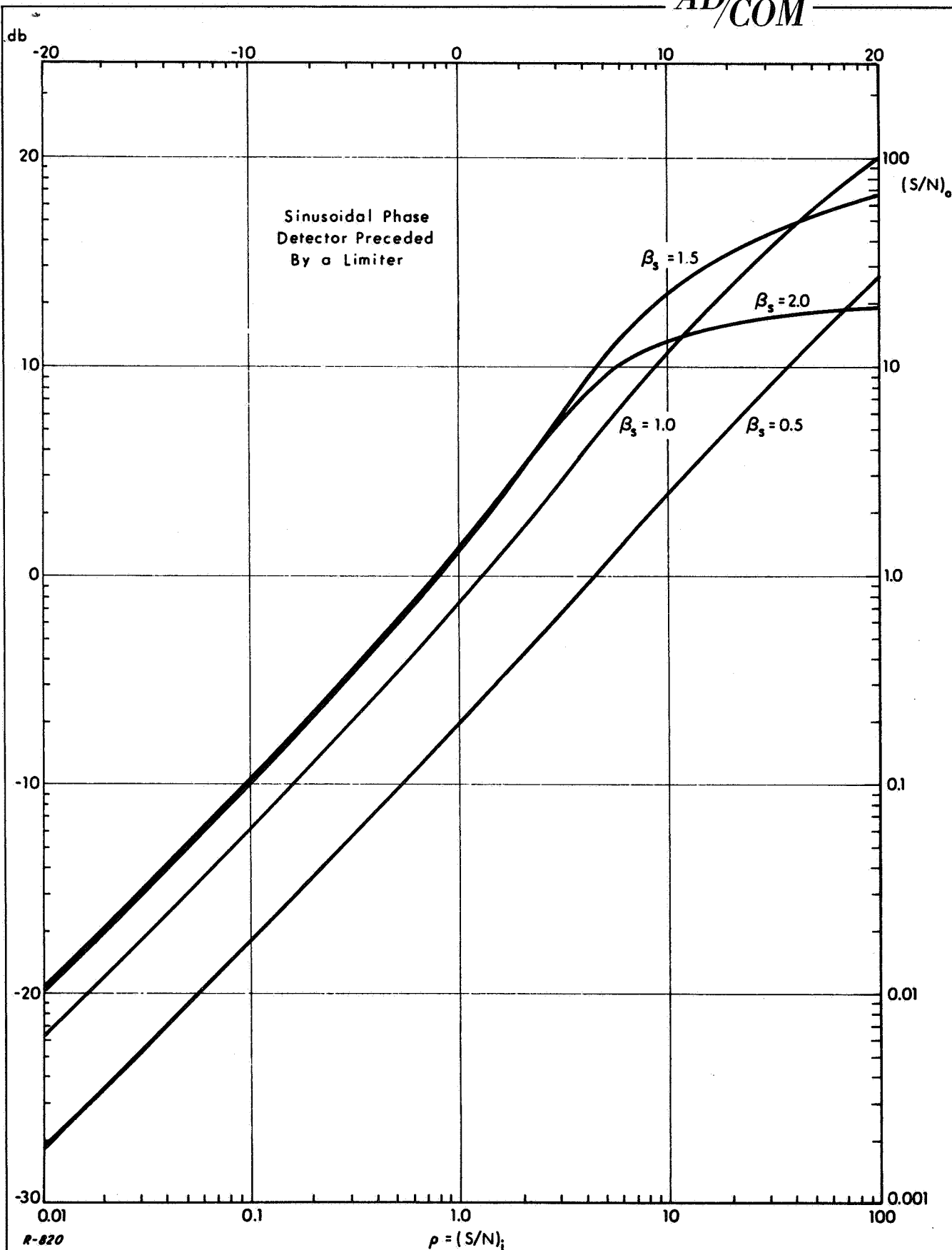


Fig. 9 SNR curves for sinusoidal phase detector preceded by a limiter.

3.3 Cross-Over Detector

For the cross-over phase detector

$$\begin{aligned} T(\phi_e) &= \phi_e - 2\pi n & (2n-1)\pi \leq \phi_e \leq (2n+1)\pi \\ n &= 0, \pm 1, \pm 2, \dots \end{aligned} \quad (73)$$

This is plotted in Fig. 10. Again, we employ Eqs. (38) and (49) to compute output signal and noise powers.

3.3.1 Calculation of S_o

The first moment $m_1(\beta, \rho)$ is

$$\begin{aligned} m_1(\beta, \rho) &= \beta - 2\pi \int_{\pi-\beta}^{\pi} q(\theta_n) d\theta_n & \beta > 0 \\ &= \beta + 2\pi \int_{-\pi}^{-\pi-\beta} q(\theta_n) d\theta_n & \beta < 0 \end{aligned} \quad (74)$$

This is shown in Appendix A to be

$$m_1(\beta, \rho) = \alpha_0(\rho) \beta + \alpha_1(\rho) \sin \beta - \sum_{n=2}^{\infty} \alpha_n(\rho) I_n(\beta) \quad (75)$$

where

$$\alpha_0(\rho) = 1 - G_0(\rho) - G_1(\rho) \quad (76a)$$

$$\alpha_n(\rho) = \frac{1}{n!} G_n(\rho) \quad n \geq 1 \quad (76b)$$

$$G_n(\rho) = \int_0^{\infty} (2\rho A)^{n+1} e^{-\rho(A+1)^2} dA \quad (77)$$

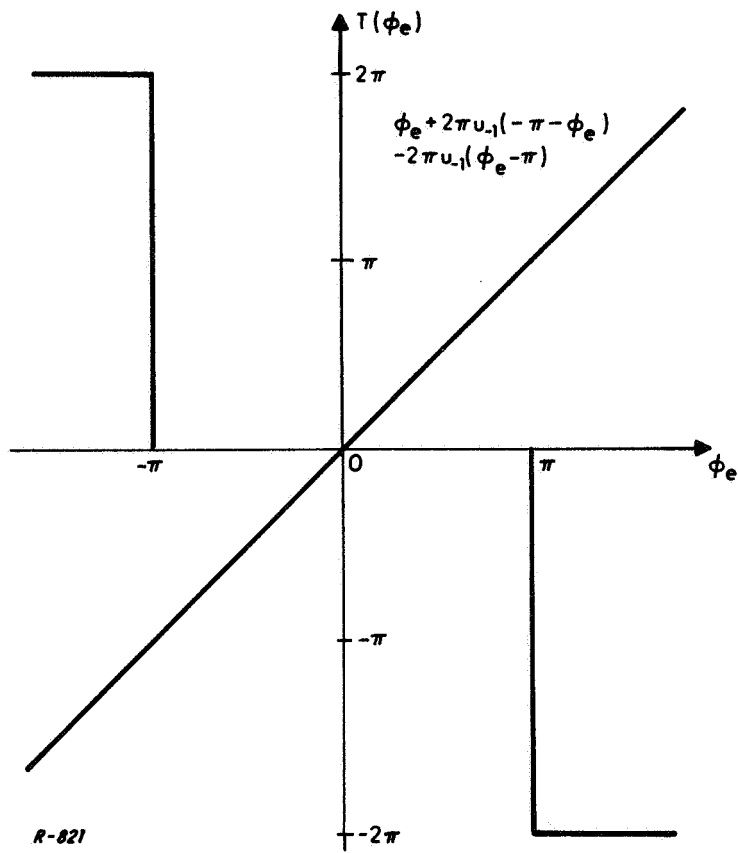
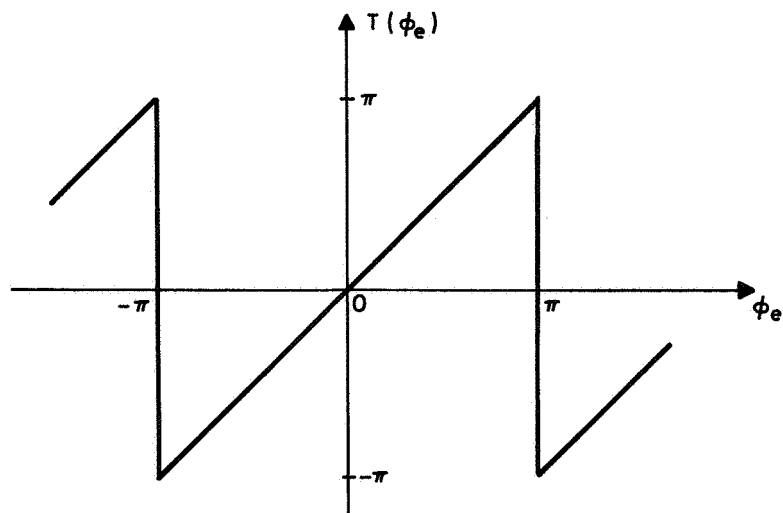


Fig. 10 Cross-over phase detector transfer function.

and

$$I_n(\beta) = \frac{1}{2^{n-1}} \sum_{k=0}^n b_{n,k} \left(\frac{\sin k \beta}{k} \right) \quad (78)$$

As shown in Appendix A, the coefficients $b_{n,k}$ and the function $G_n(\rho)$ may be obtained in a straightforward manner from simple recurrence formulas.

The significance of the terms in (75) may be appreciated from the following considerations. At large ρ , $m_1(\beta, \rho) \rightarrow \beta$ ($|\beta| \neq \pi$) and the first term in (75) dominates over a large range of β except near $|\beta| = \pi$. At small ρ , $m_1(\beta, \rho) \rightarrow \sqrt{\pi\rho} \sin \beta$, and the second term in (75) dominates. At intermediate values of ρ , the first two terms in (75) dominate at small β , but at values of β approaching $|\beta| = \pi$ the final term in (75) must be taken into account. As shown in Appendix A, the lowest power of β in a Taylor expansion of $I_n(\beta)$ about $\beta = 0$ is β^{2n+1} , and for small β only the first few terms in the sum $\sum_{n=2}^{\infty} \alpha_n(\rho) I_n(\beta)$ need be considered. This behavior is shown for $\rho = 1.0$ (0 db) in Fig. 11, where the approximation to $m_1(\beta, \rho)$ obtained by truncating the sum $\sum_{n=2}^{\infty} \alpha_n(\rho) I_n(\beta)$ in (75) is plotted over the range $0 \leq \beta \leq \pi$ for truncation at $n = 2$, $n = 4$, $n = 6$, $n = 8$, and $n = \infty$. The $n = \infty$ curve was obtained from Chadima¹. Truncation at $n = 8$ provides an adequate approximation to $m_1(\beta, \rho)$ up to $\beta = 2$ radians, which is the maximum value of β_s considered here.

Making use of (56), we may write the function $A_1(\beta_s, \rho)$ by inspection.

$$A_1(\beta_s, \rho) = \alpha_0(\rho) \beta_s + \alpha_1(\rho) 2J_1(\beta_s) - \sum_{n=2}^{\infty} \alpha_n(\rho) F_n(\beta_s) \quad (79)$$

where

$$F_n(\beta_s) = \sum_{k=0}^n \frac{1}{2^{n-1}} b_{n,k} \left(\frac{2}{k} J_1(k\beta_s) \right) \quad (80)$$

The signal power out, $S_o(\beta_s, \rho)$, is therefore

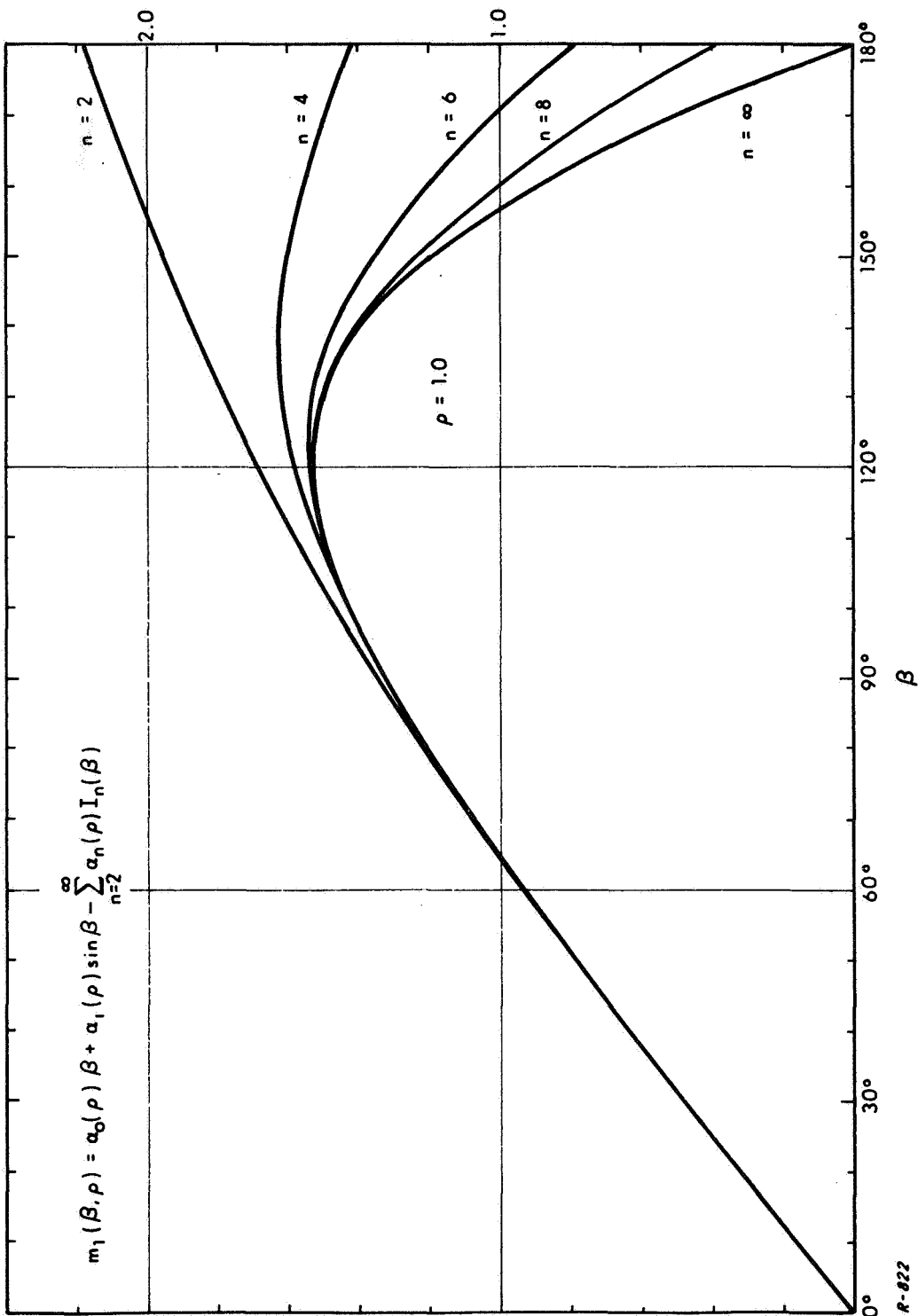


Fig. 11 Approximation of $m_1(\beta, \rho)$ obtained by truncating sum at $n = 2, 4, 6, 8, \infty$ for $\rho = 1.0$.

$$\begin{aligned}
S_o(\beta_s, \rho) &= \frac{1}{2} A_1^2(\beta_s, \rho) \\
&= \frac{1}{2} \left[\alpha_o(\rho) \beta_s + \alpha_1(\rho) 2 J_1(\beta_s) \right]^2 \\
&\quad - \left[\alpha_o(\rho) \beta_s + \alpha_1(\rho) 2 J_1(\beta_s) \right] \left(\sum_{n=2}^{\infty} \alpha_n(\rho) F_n(\beta_s) \right) \\
&\quad + \frac{1}{2} \left(\sum_{n=2}^{\infty} \alpha_n(\rho) F_n(\beta_s) \right)^2
\end{aligned} \tag{81}$$

which we write for convenience as

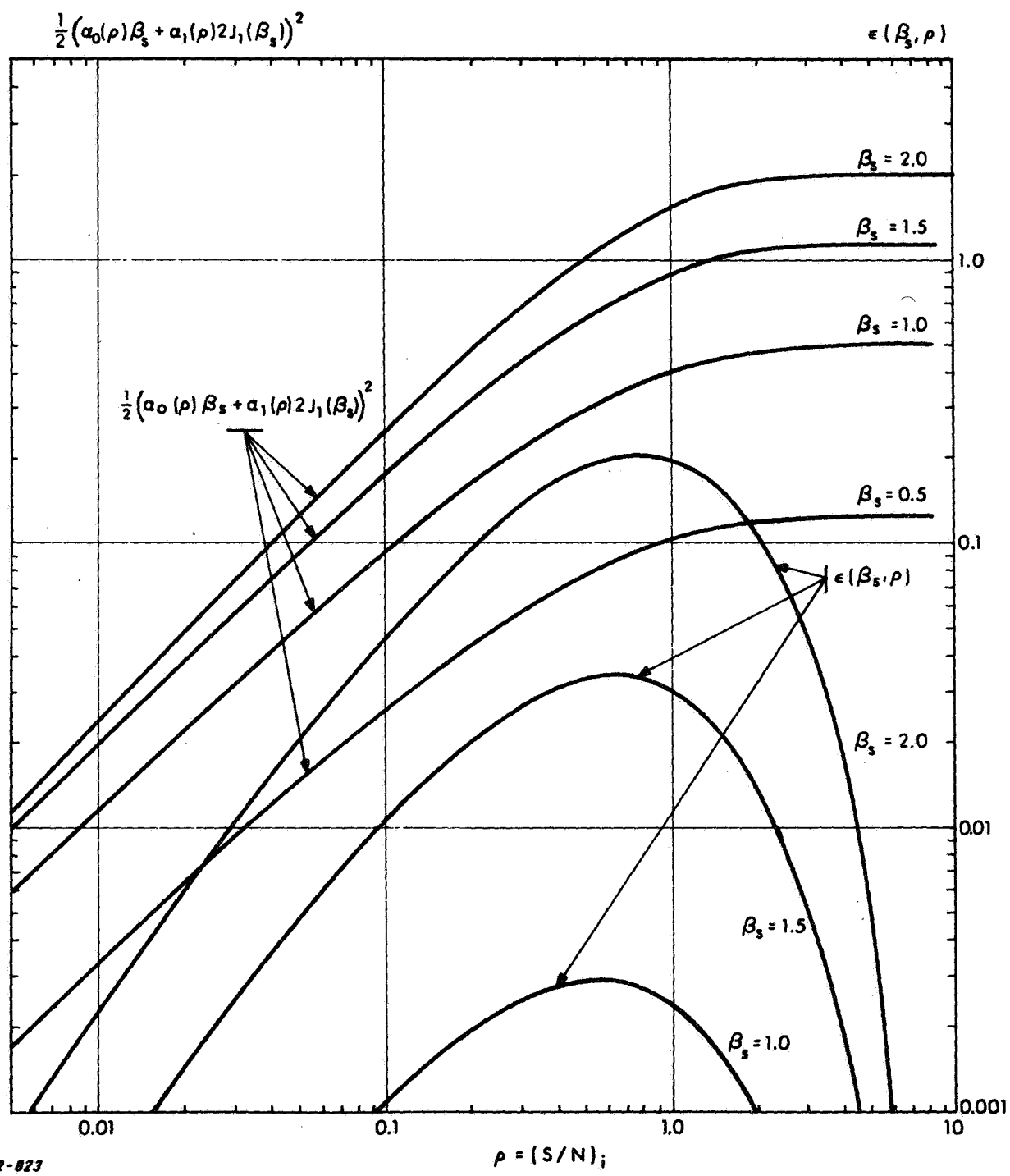
$$\begin{aligned}
S_o(\beta_s, \rho) &= \frac{1}{2} \left[\alpha_o(\rho) \beta_s + \alpha_1(\rho) 2 J_1(\beta_s) \right]^2 \\
&\quad - \epsilon(\beta_s, \rho)
\end{aligned} \tag{82}$$

The function $\epsilon(\beta_s, \rho)$ approaches zero at both low and high values of ρ . This behavior is shown in Fig. 12, where $\frac{1}{2} [\alpha_o(\rho) \beta_s + \alpha_1(\rho) 2 J_1(\beta_s)]^2$ and $\epsilon(\beta_s, \rho)$ are plotted for $\beta_s = 0.5, 1.0, 1.5,$ and 2.0 radians.

3.3.2 Calculation of N_o

For the cross-over detector, $m_2(\beta, \rho)$ is (See Fig. 13)

$$\begin{aligned}
m_2(\beta, \rho) &= \int_{-\pi}^{\pi} T^2(\beta + \theta_n) q(\theta_n) d\theta_n \\
&= \int_{-\pi}^{\pi} (\beta + \theta_n)^2 q(\theta_n) d\theta_n \\
&\quad + 4\pi^2 \int_{\pi-\beta}^{\pi} \left[1 - \frac{1}{\pi} (\beta + \theta_n) \right] q(\theta_n) d\theta_n \quad \beta > 0
\end{aligned} \tag{83}$$



R-823

Fig. 12 $\frac{1}{2}(\alpha_0(\rho)\beta_s + \alpha_1(\rho)2J_1(\beta_s))^2$ and $\epsilon(\beta_s, \rho)$.

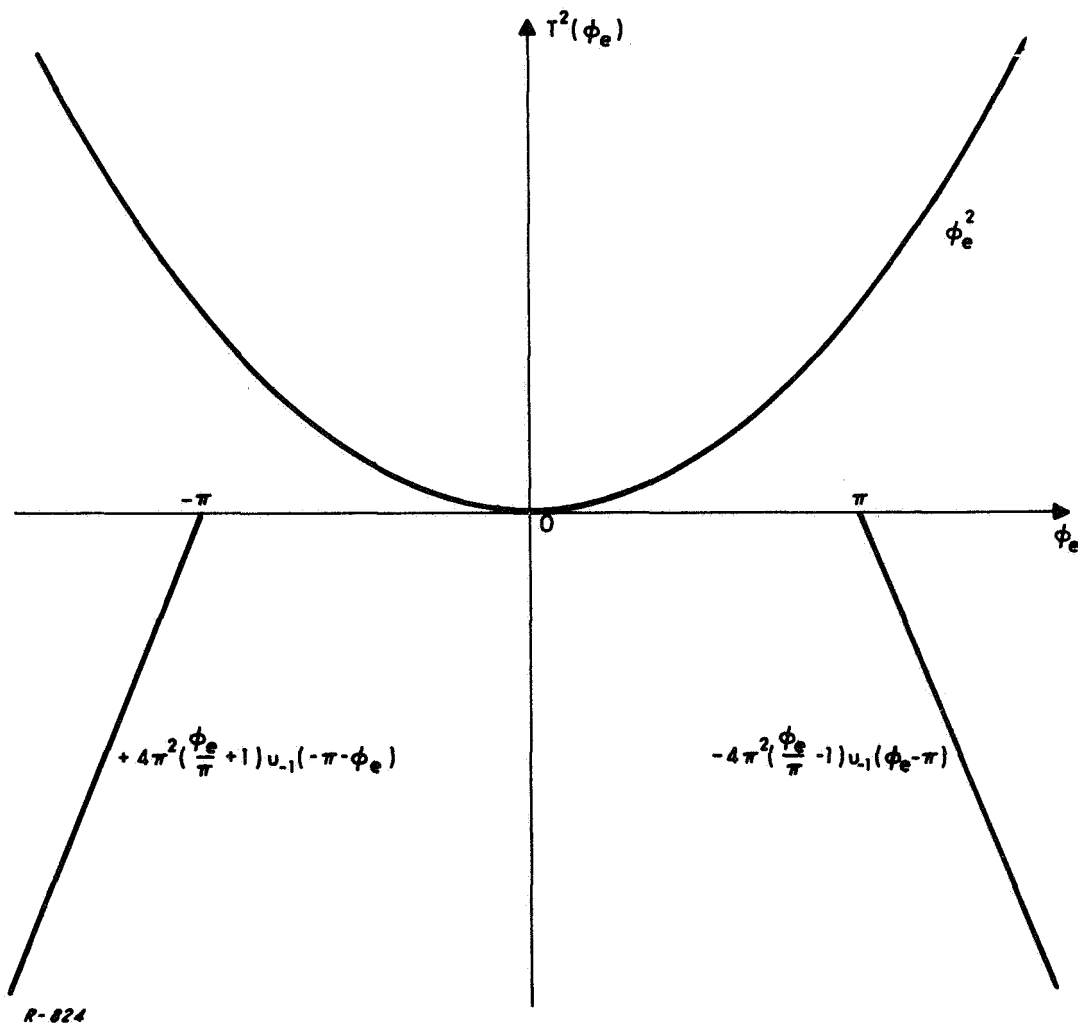
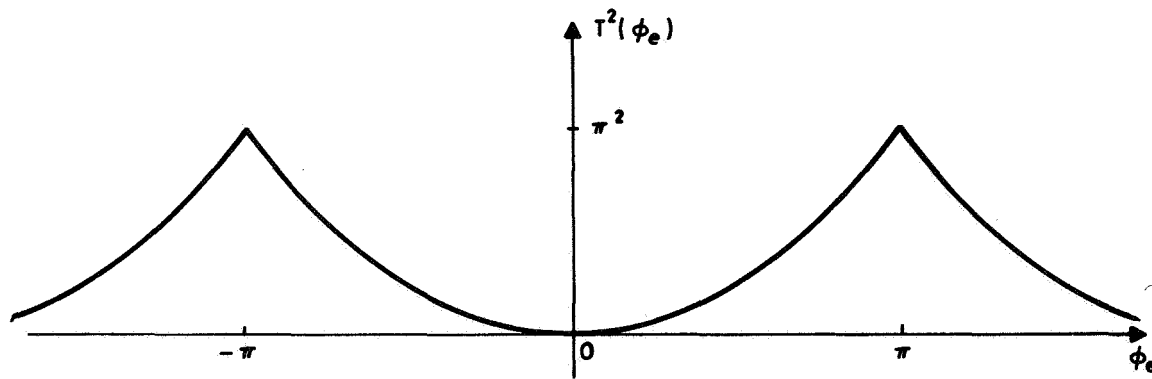


Fig. 13 Square of the cross-over phase detector transfer function.

This is shown in Appendix B to be equal to

$$m_2(\beta, \rho) = \sigma_{\theta_n}^2(\rho) + \alpha_0(\rho) \beta^2 + \alpha_1(\rho) 2(1 - \cos \beta) - 2 \sum_{n=2}^{\infty} \alpha_n(\rho) H_n(\beta) \quad (84)$$

where

$$H_n(\beta) = \sum_{k=0}^n \frac{1}{2^{n-1}} b_{n,k} \left(\frac{1 - \cos k\beta}{k^2} \right) \quad (85)$$

and where

$$\sigma_{\theta_n}^2(\rho) = \int_{-\pi}^{\pi} \theta_n^2 q(\theta_n) d\theta_n \quad (86)$$

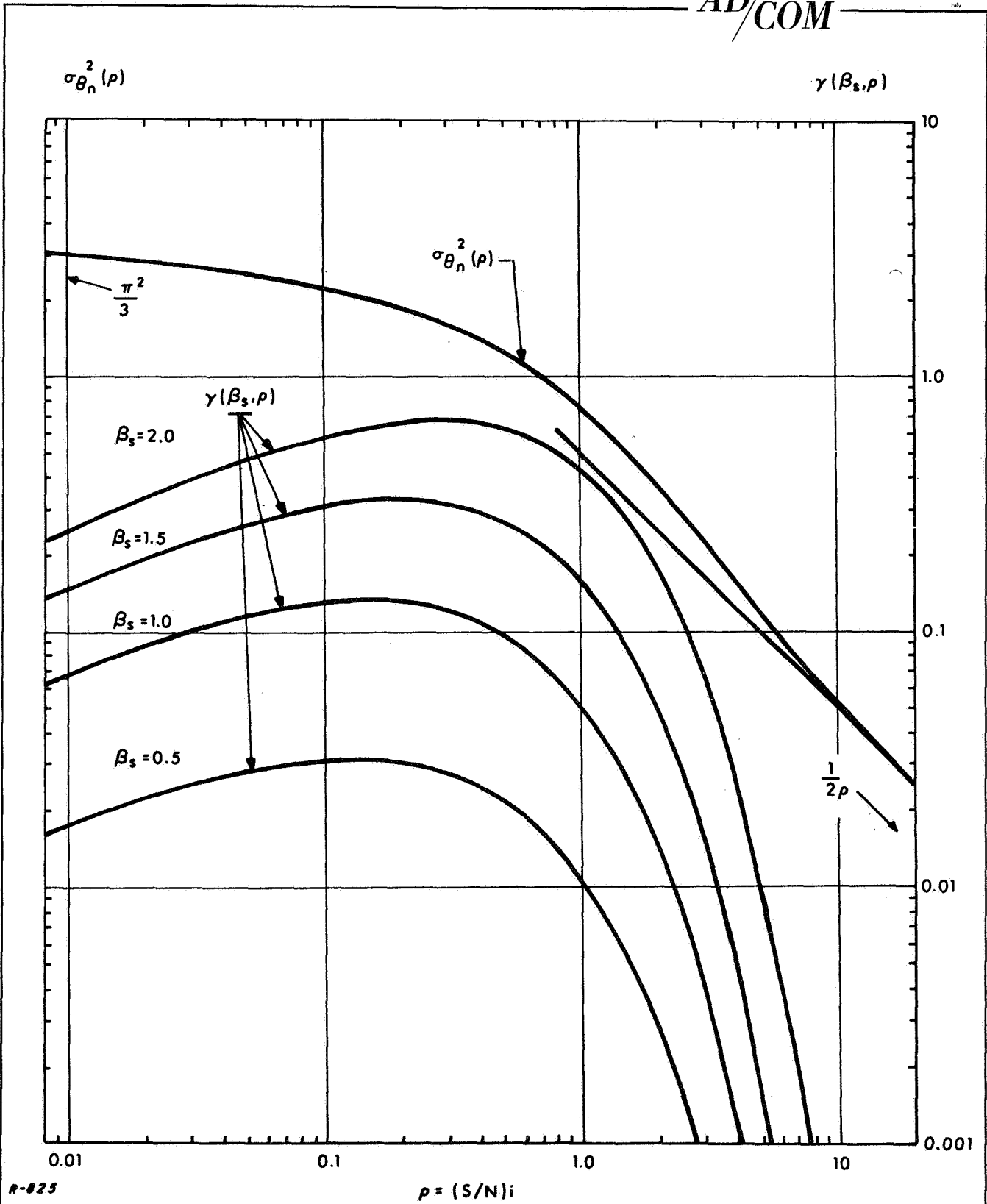
is the noise power in the absence of modulation. The function $\sigma_{\theta_n}^2(\rho)$ has been calculated by Chadima¹ and is shown plotted in Fig. 14. The asymptotic behavior of $\sigma_{\theta_n}^2$ is

$$\sigma_{\theta_n}^2(\rho \rightarrow \infty) \rightarrow \frac{1}{2\rho} \quad (87)$$

$$\sigma_{\theta_n}^2(\rho \rightarrow 0) \rightarrow \frac{\pi^2}{3} \quad (88)$$

Note that as ρ decreases below 10 (10 db) $\sigma_{\theta_n}^2(\rho)$ rises above the $1/(2\rho)$ asymptote. On the other hand, Fig. 12 shows that S_o^n deviates significantly from its high SNR asymptotic value of $1/2 \beta_s^2$ only below $\rho \approx 2$ (3 db). Thus, the cause of initial SNR degradation at approximately 10 db is the rise of $\sigma_{\theta_n}^2(\rho)$ at that value.

With $\beta = \beta_s \sin \omega_m t$, $\langle m_2(\beta_s \sin \omega_m t, \rho) \rangle_t$ becomes



R-025

Fig. 14 $\sigma_{\theta_n}^2(\rho)$ and $\gamma(\beta_s, \rho)$.

$$\begin{aligned} \langle m_2(\beta_s \sin \omega_m t, \rho) \rangle_t &= \sigma_{\theta_n}^2(\rho) + \alpha_0(\rho) \frac{1}{2} \beta_s^2 \\ &+ \alpha_1(\rho) 2 [1 - J_0(\beta_s)] - 2 \sum_{n=2}^{\infty} \alpha_n(\rho) E_n(\beta_s) \end{aligned} \quad (89)$$

where

$$E_n(\beta_s) = \sum_{k=0}^n \frac{1}{2^{n-1}} b_{n,k} \cdot \frac{[1 - J_0(k\beta_s)]}{k^2} \quad (90)$$

The noise power out, $N_o(\beta_s, \rho)$, is found from (49) to be

$$\begin{aligned} N_o(\beta_s, \rho) &= \sigma_{\theta_n}^2(\rho) + \alpha_0(\rho) \frac{1}{2} \beta_s^2 + \alpha_1(\rho) 2 [1 - J_0(\beta_s)] \\ &- 2 \sum_{n=2}^{\infty} \alpha_n(\rho) E_n(\beta_s) - S_o(\beta_s, \rho) \end{aligned} \quad (91)$$

Introducing $S_o(\beta_s, \rho)$ from (81) into (91) and regrouping terms we obtain

$$\begin{aligned} N_o(\beta_s, \rho) &= \sigma_{\theta_n}^2(\rho) + \left\{ \alpha_0(\rho) \frac{1}{2} \beta_s^2 + \alpha_1(\rho) 2 [1 - J_0(\beta_s)] \right. \\ &\quad \left. - \frac{1}{2} (\alpha_0(\rho) \beta_s + \alpha_1(\rho) 2 J_1(\beta_s))^2 \right\} \\ &+ \sum_{n=2}^{\infty} \alpha_n(\rho) \left\{ (\alpha_0(\rho) \beta_s + \alpha_1(\rho) 2 J_1(\beta_s)) F_n(\beta_s) - 2 E_n(\beta_s) \right\} \\ &\quad - \frac{1}{2} \left(\sum_{n=2}^{\infty} \alpha_n(\rho) F_n(\beta_s) \right)^2 \end{aligned} \quad (92)$$

or

$$N_o(\beta_s, \rho) = \sigma_{\theta_n}^2(\rho) + \gamma(\beta_s, \rho) \quad (93)$$

where $\gamma(\beta_s, \rho)$ is that part of the noise power which disappears in the absence of modulation. At large ρ ($\rho \rightarrow \infty$) $\gamma(\beta_s, \rho) \rightarrow 0$ faster than $1/(2\rho)$, which is how $\sigma_{\theta_n}^2(\rho)$ approaches zero, while at small ρ ($\rho \rightarrow 0$) $\gamma(\beta_s, \rho) \rightarrow \sqrt{\pi\rho} 2[1 - J_0(\beta_s)]$, which is negligible compared to $\sigma_{\theta_n}^2(\rho \rightarrow 0) = \pi^2/3$. Hence $\gamma(\beta_s, \rho)$ is only of significance at intermediate values of ρ . This behavior is also illustrated in Fig. 14, where $\gamma(\beta_s, \rho)$ is plotted as a function of ρ for $\beta_s = 0.5, 1.0, 1.5$, and 2.0 radians. The summation over n in (90) is truncated at $n=8$, which is an adequate approximation for $\beta_s \leq 2$ radians.

The output signal-to-noise ratio $(S/N)_o$ is

$$(S/N)_o = \frac{\frac{1}{2}(\alpha_0(\rho)\beta_s + \alpha_1(\rho) 2 J_1(\beta_s))^2 - \epsilon(\beta_s, \rho)}{\sigma_{\theta_n}^2(\rho) + \gamma(\beta_s, \rho)} \quad (94)$$

This is plotted as a function of ρ for $\beta_s = 0.5, 1.0, 1.5$ and 2.0 radians in Fig. 15. The asymptotic behavior of $(S/N)_o$ for the cross-over detector at large and small ρ is

$$(S/N)_o (\rho \rightarrow \infty) \rightarrow \rho \beta_s^2 \quad (95)$$

and

$$(S/N)_o (\rho \rightarrow 0) \rightarrow \frac{6}{\pi} \rho J_1^2(\beta_s) \quad (96)$$

Note that as $\rho \rightarrow 0$, $(S/N)_o$ for the cross-over detector is lower than for the sinusoidal detector preceded by a limiter at the same value of ρ . A detailed comparison of the cross-over detector with the sinusoidal detector and the conventional multiplier is presented in Sec. 3.5.

3.4 Conventional Multiplier as a Phase Detector

The conventional multiplier has no limiter. The IF signal plus additive narrowband gaussian noise is multiplied by a reference carrier, which

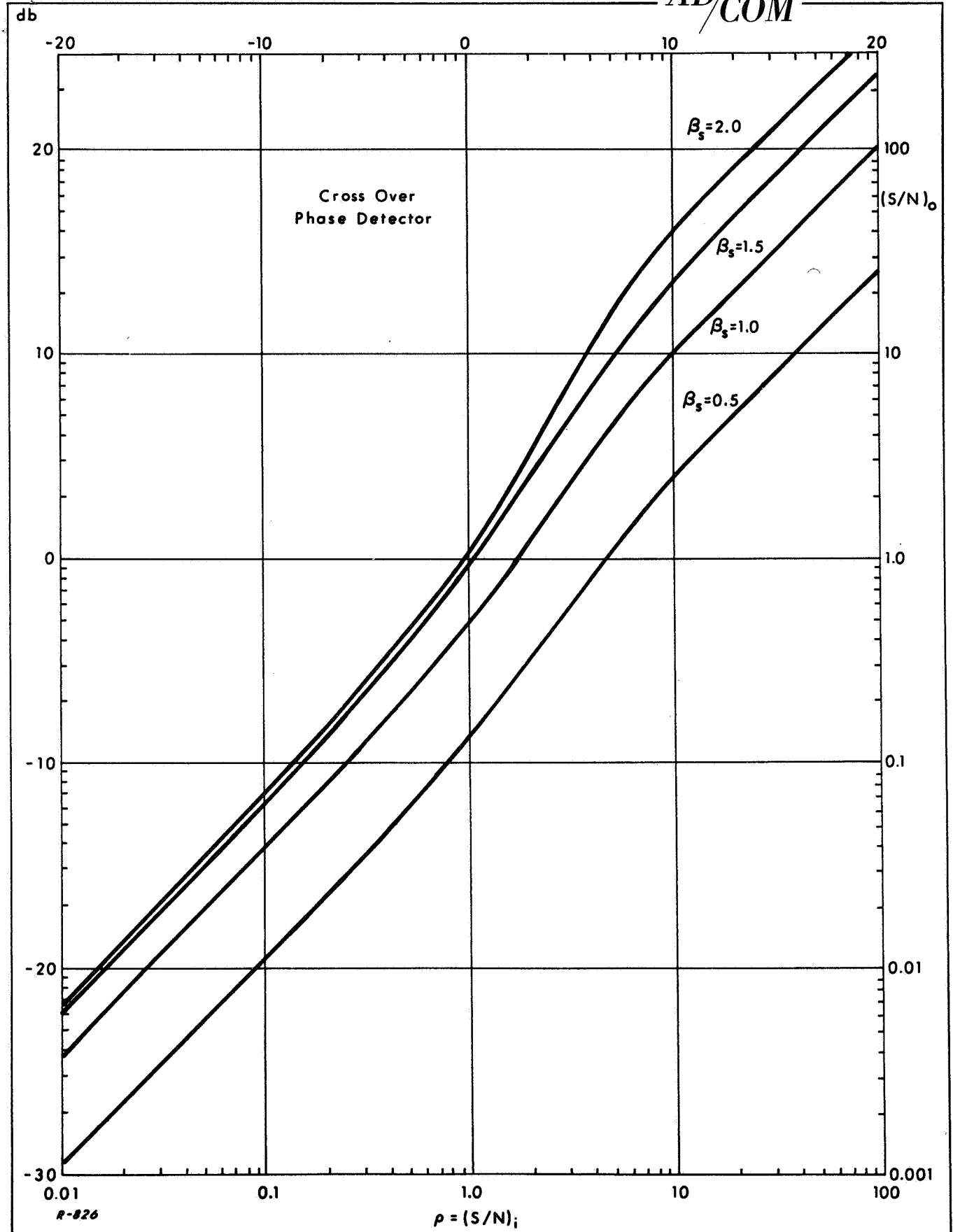


Fig. 15 SNR curves for cross-over phase detector.

we shall assume properly phased and jitter-free, and the resultant product is low-pass filtered to remove all frequency components near $2\omega_c$.

The input signal plus noise may be written as

$$e_{in}(t) = E_s \sin [\omega_c t + \beta(t)] + N_c(t) \sin [\omega_c t] + N_q(t) \cos [\omega_c t] \quad (97)$$

The reference carrier is written as

$$e_{ref}(t) = 2 \cos [\omega_c t] \quad (98)$$

The product of $e_{in}(t)$ and $e_{ref}(t)$ is

$$e_{in}(t) \cdot e_{ref}(t) = 2E_s \sin [\omega_c t + \beta(t)] \cos [\omega_c t] + 2N_c(t) \sin [\omega_c t] \cos [\omega_c t] + 2N_q(t) \cos^2 [\omega_c t] \quad (99)$$

or

$$e_{in}(t) \cdot e_{ref}(t) = E_s \sin [\beta(t)] + N_q(t) + E_s \sin [2\omega_c t + \beta(t)] + N_c(t) \sin [2\omega_c t] + N_q(t) \cos [2\omega_c t] \quad (100)$$

After filtering to remove terms near $2\omega_c$, we have the normalized output signal plus noise

$$e_o(t) = \left\{ \sin [\beta(t)] + \frac{N_q(t)}{E_s} \right\} \quad (101)$$

With $\beta(t) = \beta_s \sin \omega_m t$, $e_o(t)$ becomes

$$e_o(t) = 2J_1(\beta_s) \sin \omega_m t + 2 \sum_{\substack{n=3,5,\dots \\ (n\text{-odd})}} J_n(\beta_s) \sin n\omega_m t + \frac{N_q(t)}{E_s} \quad (102)$$

Note that the noise at the output of the multiplier phase detector is additive and gaussian. There is no signal suppression factor here as in the case of a phase detector preceded by a limiter. The signal power out, is simply

$$S_o(\beta_s, \rho) = 2J_1^2(\beta_s) \quad (103)$$

for all ρ . The noise power, N_o , is

$$N_o(\beta_s, \rho) = 2 \sum_{\substack{n=3,5,\dots \\ (n\text{-odd})}} J_n^2(\beta_s) + \frac{\langle N_q^2(t) \rangle}{E_s^2} \quad (104)$$

Since

$$\frac{\langle N_q^2(t) \rangle}{E_s^2} = \frac{\sigma_N^2}{E_s^2} = \frac{1}{2\rho} \quad (105)$$

$$N_o(\beta_s, \rho) = 2 \sum_{\substack{n=3,5,\dots \\ (n\text{-odd})}} J_n^2(\beta_s) + \frac{1}{2\rho} \quad (106)$$

The first term in (106) is just the power lying at higher harmonics of ω_m which results from the nonlinearity $\sin[\beta(t)]$. The second term is the noise power resulting from the additive gaussian noise, and is the total noise power out in the absence of modulation.

The signal-to-noise ratio out is therefore

$$(S/N)_o = \frac{2J_1^2(\beta_s)}{2 \sum_{\substack{n=3,5,\dots \\ (n\text{-odd})}} J_n^2(\beta_s) + \frac{1}{2\rho}} \quad (107)$$

This is plotted as a function of ρ for $\beta_s = 0.5, 1.0, 1.5,$ and 2.0 radians in Fig. 16. The asymptotic behavior of $(S/N)_o$ in the limit of large and small ρ is

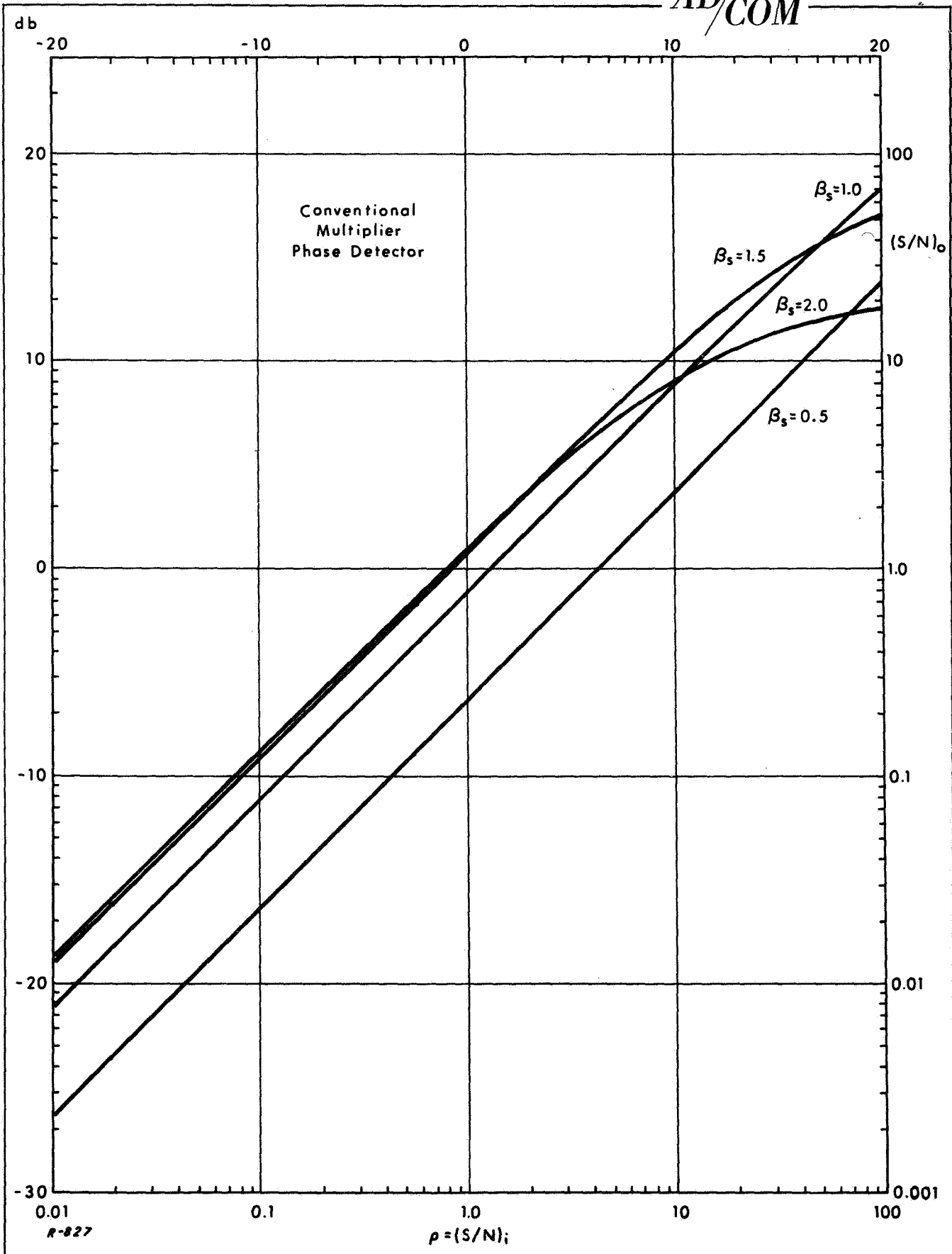


Fig. 16 SNR curves for the conventional multiplier.

$$(S/N)_o (\rho \rightarrow \infty) \rightarrow \frac{J_1^2(\beta_s)}{\sum_{n=3,5,\dots} J_n^2(\beta_s)} \quad (108)$$

and

$$(S/N)_o (\rho \rightarrow 0) \rightarrow 4\rho J_1^2(\beta_s) \quad (109)$$

The behavior at large ρ is the same as for the case of the sinusoidal phase detector preceded by a limiter in that the nonlinearity of $\sin \beta$ limits the output signal-to-noise ratio as $\rho \rightarrow \infty$. As $\rho \rightarrow 0$ the output signal-to-noise ratio is larger than for either the cross-over detector or the sinusoidal phase detector preceded by a limiter. The signal-to-noise ratios out for the three phase detectors are compared in more detail in the next section.

3.5 Comparison of the SNR Behavior of the Three Phase Detectors

To compare the SNR behavior of the three phase detectors, we plot the SNR curves at fixed β_s for each of the three phase detectors in the same figure. This is shown in Figs. 17, 18, 19, and 20 for $\beta_s = 0.5, 1.0, 1.5$ and 2.0 radians respectively. Points at which the SNR curves intersect are circled.

Examination of these figures indicates that no one phase detector may be considered as best at all values of ρ . In particular, at low input SNR, it is found that the conventional multiplier has the best SNR behavior, followed by the sinusoidal phase detector and the cross-over detector in that order. This is predicted by the asymptotic behavior of the $(S/N)_o$ functions at low input SNR indicated below.

Conventional Multiplier:

$$(S/N)_o (\rho \rightarrow 0) \rightarrow (4) \rho J_1^2(\beta_s) \quad (110)$$

Sinusoidal Phase Detector Preceded By Limiter:

$$(S/N)_o (\rho \rightarrow 0) \rightarrow (\pi) \rho J_1^2(\beta_s) \quad (111)$$

Cross-Over Detector:

$$(S/N)_o (\rho \rightarrow 0) \rightarrow (6/\pi) \rho J_1^2(\beta_s) \quad (112)$$

At high input SNR, on the other hand, the situation is just the reverse of that for low input SNR. Here the cross-over detector has the best SNR behavior, followed by the sinusoidal phase detector and the conventional multiplier in that order. This is most noticeable at the larger values of β_s . This is also predicted by the asymptotic behavior of the $(S/N)_o$ functions at high input SNR indicated below.

Cross-Over Detector:

$$(S/N)_o (\rho \rightarrow \infty) \rightarrow \rho \beta_s^2 \quad (113)$$

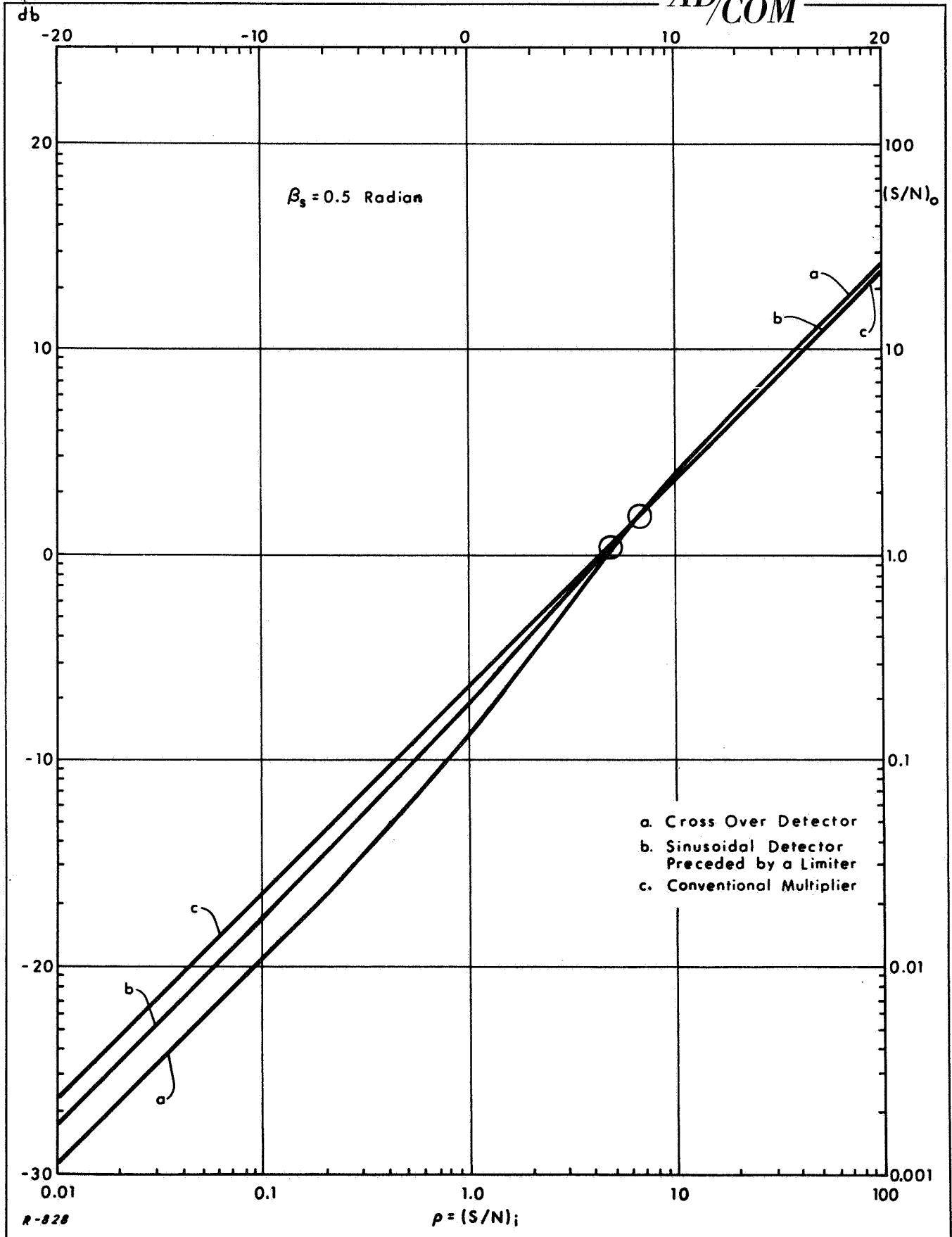


Fig. 17 Comparison of the SNR curves of the three phase detectors for $\beta_s = 0.5$ rad.

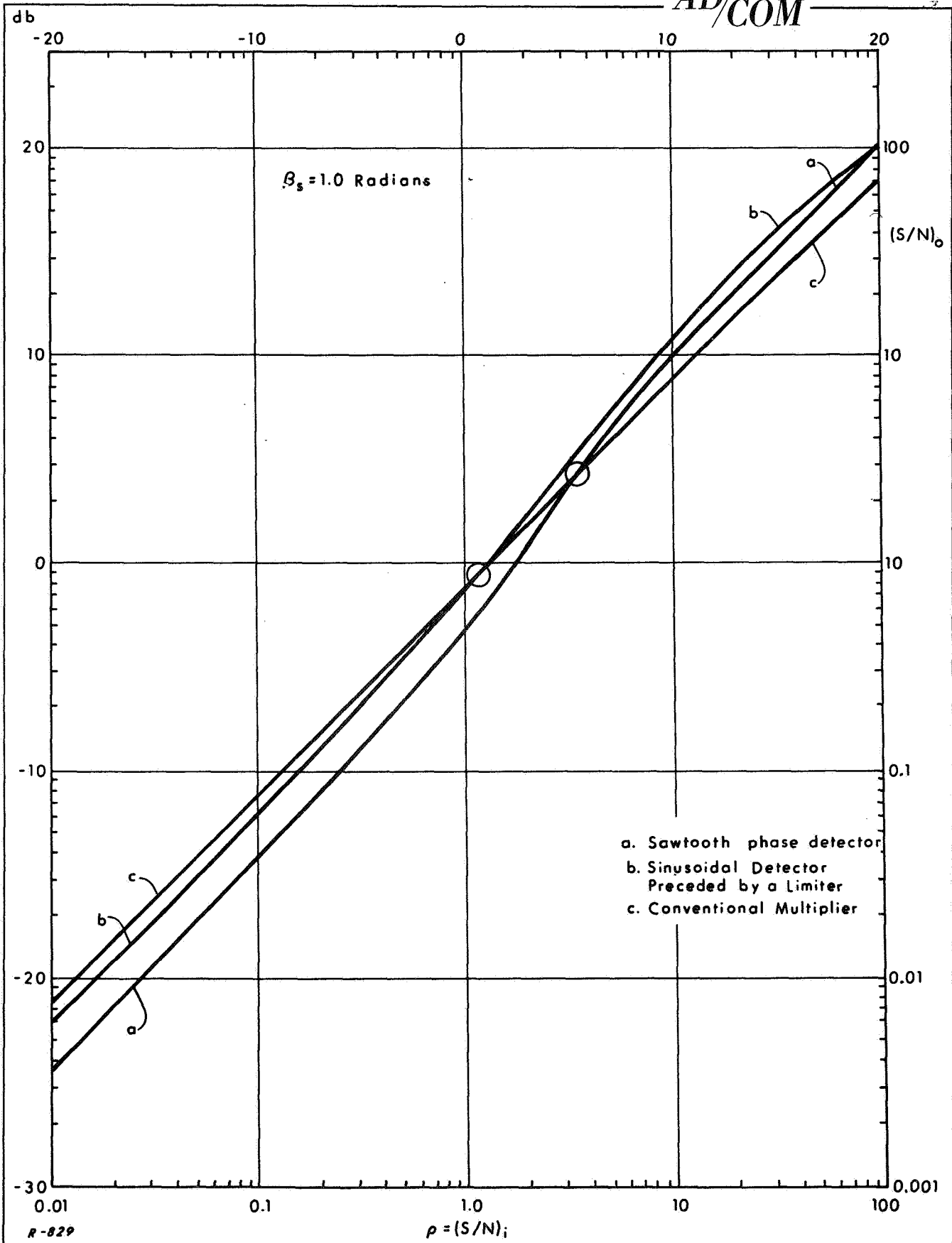


Fig. 18 Comparison of the SNR curves of the three phase detectors for $\beta_s = 1.0$ rad.

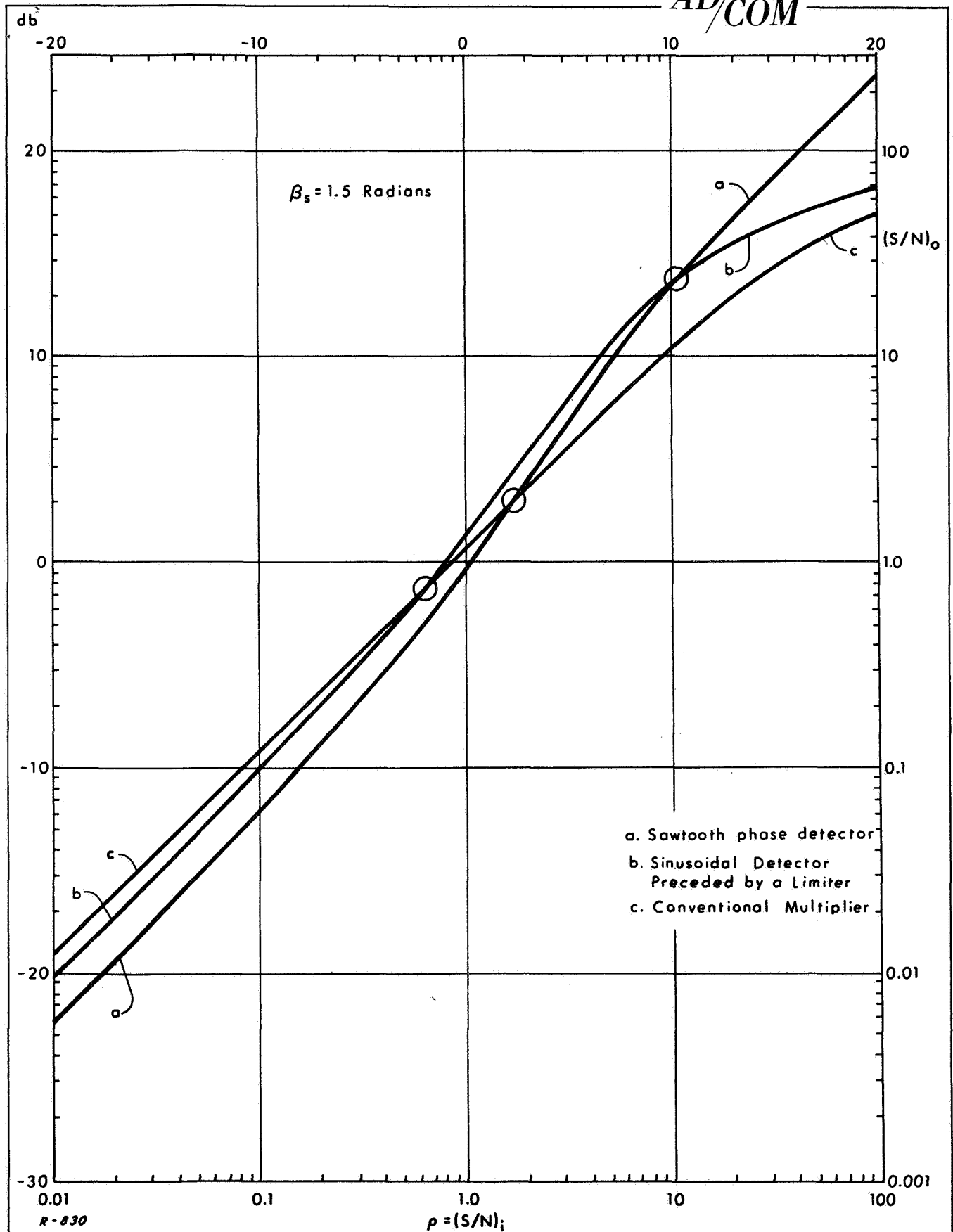


Fig. 19 Comparison of the SNR curves of the three phase detectors for $\beta_s = 1.5$ rads.

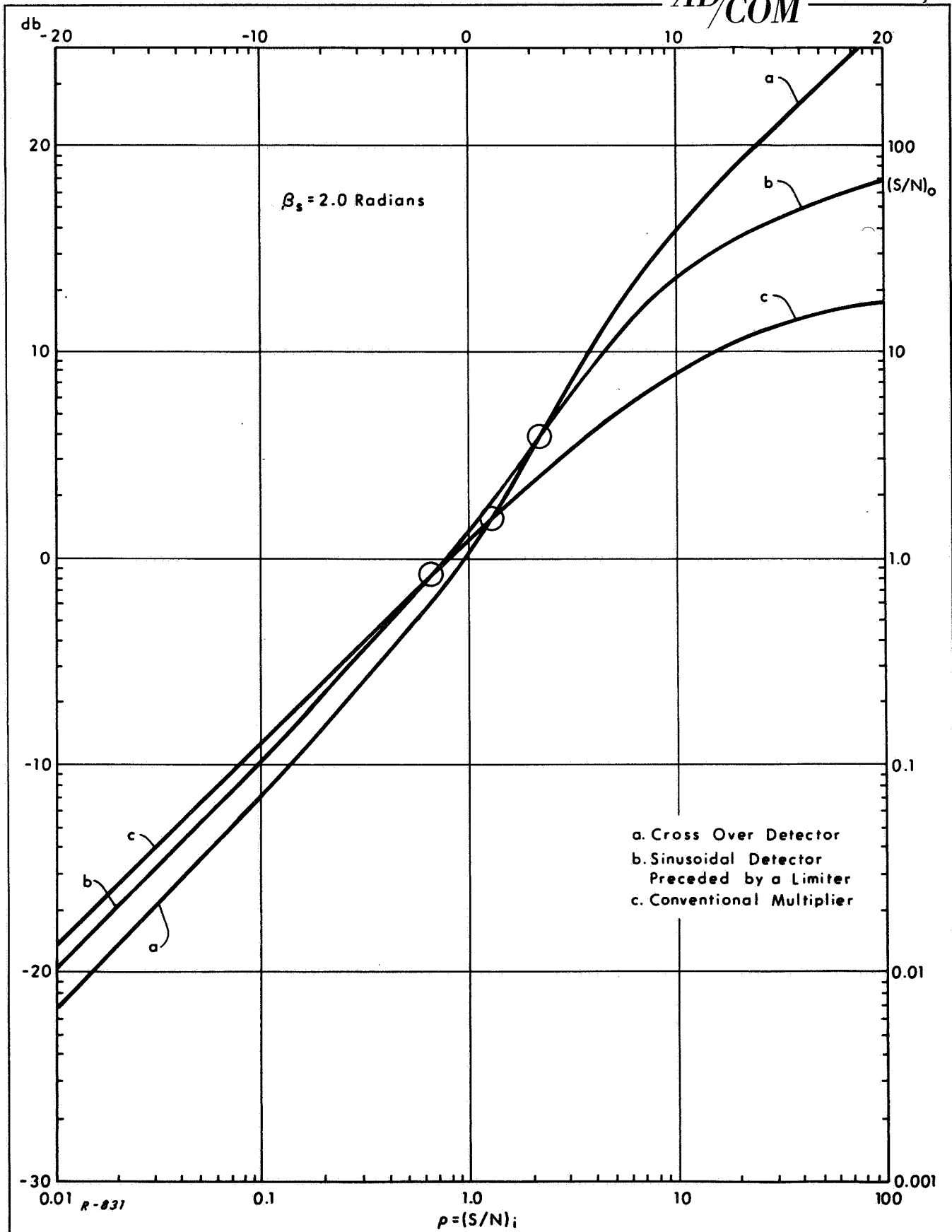


Fig. 20 Comparison of the SNR curves of the three phase detectors for $\beta_s = 2.0$ rads.

Sinusoidal Phase Detector preceded by limiter:

$$(S/N)_O (\rho \rightarrow \infty) \rightarrow \frac{2J_1^2(\beta_s)}{\left(\frac{1}{2\rho}\right) \left[J_0^2(2\beta_s) + 2J_1^2(\beta_s) \right] + 2 \sum_{n=3,5,\dots} J_n^2(\beta_s)} \quad (114)$$

Conventional Multiplier:

$$(S/N)_O (\rho \rightarrow \infty) \rightarrow \frac{2J_1^2(\beta_s)}{\left(\frac{1}{2\rho}\right) + 2 \sum_{n=3,5,\dots} J_n^2(\beta_s)} \quad (115)$$

Note that as ρ becomes so large that

$$\frac{1}{2\rho} \ll 2 \sum_{n=3,5,\dots} J_n^2(\beta_s) \quad (116)$$

(114) and (115) both approach

$$(S/N)_O (\rho \rightarrow \infty) \rightarrow \frac{J_1^2(\beta_s)}{\sum_{n=3,5,\dots} J_n^2(\beta_s)} \quad (117)$$

The noise in this case consists entirely of distortion harmonics at $3\omega_m, 5\omega_m$ etc. This behavior is most noticeable for the $\beta_s = 2.0$ radians case of Fig. 20.

Note also that for ρ large enough so that (113), (114), and (115) are valid approximations for $(S/N)_O$, but for β_s small enough so that

$$\frac{1}{2\rho} \gg 2 \sum_{n=3,5,\dots} J_n^2(\beta_s) \quad (118)$$

the $(S/N)_O$ curves may be approximated by

$$\text{Cross-Over Detector: } (S/N)_O \approx \rho \beta_s^2 \quad (119)$$

Sinusoidal Phase Detector:

$$(S/N)_o \approx \frac{\rho 4J_1^2(\beta_s)}{(1 - \frac{1}{2}\beta_s^2)} \approx \rho \beta_s^2 (1 + \frac{1}{4}\beta_s^2) \quad (120)$$

$$\text{Conventional Multiplier: } (S/N)_o \approx \rho 4J_1^2(\beta_s) \approx \rho \beta_s^2 (1 - \frac{\beta_s^2}{4}) \quad (121)$$

In this case, the SNR curves are linear functions of ρ , and the cross-over detector is actually the best of the three phase detectors. This behavior is most evident in the $\beta_s = 0.5$ radian case of Fig. 17 for $\rho > 10$.

IV. CONCLUSIONS

We have computed the SNR behavior of three commonly used coherent phase detectors, under conditions of sinusoidal modulation and additive narrow band gaussian noise. The local reference carrier was assumed to be correctly phased and jitter-free. Results were obtained over a wide range of input SNR, including the intermediate or threshold region 0 db to 10 db. Output noise power was considered to be measured in the presence of modulation with the aid of a notch filter, so that any harmonic distortion components were included in the noise. Several explicit conclusions may be drawn from the resulting SNR curves:

- a) Both the cross-over detector and the sinusoidal detector preceded by a limiter exhibit a threshold effect in the range $\rho = 0$ to 10 db.
- b) This threshold effect is more pronounced for higher phase deviations β_s .
- c) The conventional multiplier exhibits no threshold effect.
- d) All the SNR curves maintain unity slope in the low SNR range. Stated equivalently, SNR degradation below threshold is gradual, rather than catastrophic as in FM demodulators. This is a property of coherent detectors. Jitter on the carrier reference would tend to increase the SNR degradation at low ρ .
- e) Noise power measured in the presence of modulation is always greater than that measured in its absence. Part of the difference is the power in the harmonic distortion.
- f) Both the conventional multiplier and the sinusoidal detector preceded by a limiter produce high harmonic distortion for β_s greater than one radian, even in the absence of noise.
- g) The cross-over detector produces no distortion in the absence of noise, even for β_s approaching π radians. As input SNR decreases, distortion increases. For a given input SNR, the distortion increases with deviation.

- h) At low input SNR the conventional multiplier has the best SNR behavior, followed by the sinusoidal phase detector then the cross-over detector.
- i) At high SNR the cross-over detector has the best SNR behavior, followed by the sinusoidal phase detector then the conventional multiplier.
- j) At high SNR and high deviation, the cross-over detector is significantly better than the other two detectors which suffer from high distortion and suppression of the fundamental modulation component.
- k) At high SNR and low deviation such that inequality (118) holds, all detectors yield equivalent performance.

In a practical situation, the system designer would have a definite transmitter power and receiver noise power density. In the case of sinusoidal modulation, the designer would have at his disposal the choices of phase deviation and type of phase detector to be used in the receiver. For the sinusoidal phase detector or the conventional multiplier, the largest value of β_s that should be used is 1.84 radians, which corresponds to the maximum of $J_1(\beta_s)$. Any value larger than this produces an output SNR curve which lies lower than the SNR curve for 1.84 radians at all values of ρ . A value of β_s larger than 1.84 radians can be used with the cross-over detector, however, and an improvement over the sinusoidal phase detector with $\beta_s = 1.84$ radians may be realized at high input SNR. If β_s for the cross-over detector is made much larger than 1.84 radians, the IF filter bandwidth may have to be widened to accommodate the larger IF signal bandwidth. This would introduce more input noise power, of course. The main advantage of the cross-over detector over the other two detectors is that at high values of ρ larger deviations can be used with little distortion.

The analysis and results of this report apply to coherent phase demodulators employing a perfect carrier reference. They also apply to phase demodulators that extract the carrier reference by means of a narrow-band carrier-tracking phase-locked loop, except that the residual carrier phase jitter will degrade the predicted performance at very low input SNR. However, they do not apply directly to modulation-tracking phase-locked loops.

We have intentionally ignored post-detection filtering in the analysis, in order to concentrate attention on the phase detectors themselves. Accordingly, we calculated the output noise power over an unbounded bandwidth. Now, in simulating a signal by a test tone, it is customary to choose the tone frequency, ω_m , well below the highest allowable modulation frequency, and hence much smaller than the IF bandwidth. In such cases most of the output noise power will be concentrated in a video band not much wider than half the IF bandwidth. A post-detection filter whose bandwidth is of the order of half the IF bandwidth will thus not materially alter the SNR curves.

A narrower post-detection bandwidth intended to reduce the output noise power raises some new problems. If the output noise power density were relatively flat, then post-detection filtering would simply improve the output SNR by a fixed amount at all values of input SNR. Expectedly this is not the case. The amount of SNR improvement by the filter depends not only on its transfer function, but also on the noise power-density spectrum. The latter depends in turn upon input SNR, phase deviation and modulation frequency. Evaluation of this power density spectrum is more complicated than the calculation of the total noise power.

For the case where the tone modulation represents a sinusoidal subcarrier at frequency ω_m , one would use a narrowband subcarrier filter centered at ω_m at the output of the phase detector in order to reduce the output

noise. Once again, in order to calculate the total noise power at the output of this filter, the noise power spectrum would have to be evaluated.

In conclusion, we note that the calculation of the first moment $m_1(\beta, \rho)$, from which the signal suppression for any type of modulation may be calculated is highly useful in that this signal suppression occurs independently of any post-phase detector linear filtering. The noise power results, on the other hand, characterize the total noise power at the output of the phase detector prior to any post-detection filtering. These results may not be too accurate if post-detection filtering is used, but they serve as an upper bound to the noise power at the output of a post-detection filter, since this must certainly be less than the noise power at the output of the phase detector.

The calculations are useful also in that they can readily be verified experimentally, thus confirming the validity of the various theoretical models used in the analysis.

V. PROGRAM FOR NEXT INTERVAL

The time remaining in the period of performance of the subject contract will be allocated exclusively to the completion of Task I.

Task I

Apply the available analyses of intermodulation distortion caused by phase non-linearities to cover:

- a. AM to PM conversion effects in limiters,
- b. Non-linearities in demodulators, and
- c. Overall filter design problems, e. g. , form factor vs phase linearity. In particular, a catalog of commonly used predetection filters along with their intermodulation distortion levels will be compiled.

REFERENCES

1. Chadima, G. E. , "Phase Noise Theory Applied to Detection, "
Collins Research Report No. 272, 15 March 1963.
2. Lee, Y. W. , Statistical Theory of Communication, John Wiley
& Sons, 1960, p. 235.
3. Jahnke and Emde, Tables of Functions, Dover Publications, 1945
p 280, Fig. 159, $\alpha = 1.5$.

PRECEDING PAGE BLANK NOT FILMED.

APPENDIX A

Calculation of S_o for the Cross-Over Detector

For $\beta > 0$, $m_1(\beta, \rho)$ is

$$m_1(\beta, \rho) = \beta - 2\pi \int_{\pi-\beta}^{\pi} q(\theta_n) d\theta_n \quad (A-1)$$

It is convenient to introduce the variable ϕ defined by

$$\phi = \pi - \theta_n \quad (A-2)$$

so that $m_1(\beta, \rho)$ becomes

$$m_1(\beta, \rho) = \beta - 2\pi \int_0^{\beta} q(\pi - \phi) d\phi \quad (A-3)$$

The probability density function $q(\theta_n)$ is obtained¹ by integrating the joint amplitude-phase probability density function $p_j(A, \theta_n)$ over all possible amplitudes

$$q(\theta_n) = \int_0^{\infty} p_j(A, \theta_n) dA \quad (A-4)$$

The function $p_j(A, \theta_n)$ is obtained from the vector-noise model (see Chadima¹) and is

$$p_j(A, \theta_n) = \frac{\rho}{\pi} e^{-\rho} e^{-\rho A^2} A e^{2\rho A \cos \theta_n} \quad (A-5)$$

where A is the normalized amplitude of the combined input signal plus noise (normalized to the signal amplitude E_s). Hence, $m_1(\beta, \rho)$ becomes

$$m_1(\beta, \rho) = \beta - 2\rho e^{-\rho} \int_0^{\beta} d\phi \int_0^{\infty} dA e^{-\rho A^2} A e^{-2\rho A \cos \phi} \quad (A-6)$$

It is convenient to interchange the order of integration over A and ϕ , and to integrate over ϕ first. To integrate (A-6), we rewrite the integral as

$$m_1(\beta, \rho) = \beta - \int_0^\infty (2\rho A) e^{-\rho(A+1)^2} dA \int_0^\beta e^{2\rho A(1 - \cos \phi)} d\phi \quad (\text{A-7})$$

Since the integral over ϕ cannot be evaluated in closed form, we expand $e^{2\rho A(1 - \cos \phi)}$ in an infinite series as

$$e^{2\rho A(1 - \cos \phi)} = \sum_{n=0}^{\infty} \frac{1}{n!} (2\rho A)^n (1 - \cos \phi)^n \quad (\text{A-8})$$

Now $m_1(\beta, \rho)$ becomes

$$m_1(\beta, \rho) = \beta - \sum_{n=0}^{\infty} \int_0^\infty (2\rho A)^{n+1} e^{-\rho(A+1)^2} dA \frac{1}{n!} \int_0^\beta (1 - \cos \phi)^n d\phi \quad (\text{A-9})$$

$$= \beta - \sum_{n=0}^{\infty} \frac{1}{n!} G_n(\rho) I_n(\beta) \quad (\text{A-10})$$

where we have defined

$$G_n(\rho) = \int_0^\infty (2\rho A)^{n+1} e^{-\rho(A+1)^2} dA \quad (\text{A-11})$$

and

$$I_n(\beta) = \int_0^\beta (1 - \cos \phi)^n d\phi \quad (\text{A-12})$$

For $n = 0$, and $n = 1$

$$I_0(\beta) = \beta \quad (\text{A-13})$$

and

$$I_1(\beta) = \beta - \sin \beta \quad (\text{A-14})$$

For $n \geq 2$ we expand $(1 - \cos \phi)^n$ as

$$(1 - \cos \phi)^n = \sum_{k=0}^n \frac{1}{2^{n-1}} b_{n,k} \cos k\phi \quad (\text{A-15})$$

so that $I_n(\beta)$ becomes

$$I_n(\beta) = \sum_{k=0}^n \frac{1}{2^{n-1}} b_{n,k} \left(\frac{\sin k\beta}{k} \right) \quad n \geq 2 \quad (\text{A-16})$$

The coefficients $b_{n,k}$ are obtained by writing

$$(1 - \cos \phi)^n = (1 - \cos \phi)^{n-1} (1 - \cos \phi) \quad (\text{A-17})$$

or

$$\begin{aligned} \sum_{k=0}^n \frac{1}{2^{n-1}} b_{n,k} \cos k\phi &= \sum_{k=0}^{n-1} \frac{1}{2^{n-2}} b_{n-1,k} \cos k\phi \\ &- \sum_{k=0}^{n-1} \frac{1}{2^{n-2}} b_{n-1,k} \cos k\phi \cos \phi \end{aligned} \quad (\text{A-18})$$

Using the relationship

$$\cos k\phi \cos \phi = \frac{1}{2} \cos (k+1)\phi + \frac{1}{2} \cos (k-1)\phi \quad (\text{A-19})$$

(A-18) becomes

$$\begin{aligned} \sum_{k=0}^n \frac{b_{n,k}}{2^{n-1}} \cos k\phi &= \sum_{k=0}^{n-1} \frac{2b_{n-1,k}}{2^{n-1}} \cos k\phi - \sum_{k=0}^{n-1} \frac{b_{n-1,k}}{2^{n-1}} \cos (k+1)\phi \\ &- \sum_{k=0}^{n-1} \frac{b_{n-1,k}}{2^{n-1}} \cos (k-1)\phi \end{aligned} \quad (\text{A-20})$$

Equating coefficients of $\cos k\phi$, we obtain

$$(k=0) \quad b_{n,0} = 2b_{n-1,0} - b_{n-1,1} \quad (\text{A-21})$$

(k=1)

$$b_{n,1} = 2b_{n-1,1} - 2b_{n-1,0} - b_{n-1,2} \quad (\text{A-22})$$

(k=n)

$$b_{n,n} = -b_{n-1,n-1} \quad (\text{A-23})$$

(k=n-1)

$$b_{n,n-1} = 2b_{n-1,n-1} - b_{n-1,n-2} \quad (\text{A-24})$$

(all other k)

$$b_{n,k} = 2b_{n-1,k} - b_{n-1,k-1} - b_{n-1,k+1} \quad (\text{A-25})$$

With $b_{1,0} = 1$ and $b_{1,1} = -1$ the coefficients $b_{n,k}$ for $k = 2, 3, 4, 5, 6, 7$, and 8 are easily obtained from (A-21) through (A-25), and are listed in Table A-1.

Table A-1

Coefficients $b_{n,k}$ up to $n = 8$

n, k	0	1	2	3	4	5	6	7	8
2	3	-4	1						
3	10	-15	6	-1					
4	35	-56	28	-8	1				
5	126	-210	120	-45	10	-1			
6	462	-792	495	-220	66	-12	1		
7	1716	-3003	2002	-1001	364	-91	14	-1	
8	6435	-9724	8008	-4368	1820	-560	120	116	1

Referring to (A-12), we note that since the leading term in a Taylor series expansion of $(1 - \cos \phi)^n$ is $(\phi^2/2)^n$, the leading term in $I_n(\beta)$ is β^{2n+1} . Hence for small β , the terms $\sum_{n=2}^{\infty} \frac{1}{n!} G_n(\rho) I_n(\beta)$ will be negligible compared to the leading terms $(1 - G_0(\rho) - G_1(\rho))\beta + G_1(\rho) \sin \beta$ of (A-10). This behavior is

illustrated in Fig. 6 where for $\rho = 1$ successive approximations to $m_1(\beta, \rho)$ obtained by truncating the above sum at $n = 2, 4, 6, 8,$ and ∞ are plotted.

We now turn our attention to $G_n(\rho)$. Note that $G_n(\rho)$ defined in (A-11) may be written as

$$G_n(\rho) = \int_0^{\infty} (2\rho A)^n 2\rho(A+1) e^{-\rho(A+1)^2} dA - 2\rho \int_0^{\infty} (2\rho A)^n e^{-\rho(A+1)^2} dA \quad (\text{A-26})$$

The second integral is recognized as $2\rho G_{n-1}(\rho)$. The first integral may be integrated by parts as follows

$$\begin{aligned} u &= -(2\rho A)^n, \quad dv = -2\rho(A+1) e^{-\rho(A+1)^2} dA \\ du &= -2\rho n (2\rho A)^{n-1} dA, \quad v = e^{-\rho(A+1)^2} \\ \int_0^{\infty} u dv &= uv \Big|_0^{\infty} - \int_0^{\infty} v du \\ &= -(2\rho A)^n e^{-\rho(A+1)^2} \Big|_0^{\infty} + 2\rho n \int_0^{\infty} (2\rho A)^{n-1} e^{-\rho(A+1)^2} dA \\ &= 2\rho n G_{n-2}(\rho) \quad n \geq 1 \end{aligned} \quad (\text{A-27})$$

$$= e^{-\rho} - 2\rho \int_0^{\infty} e^{-\rho(A+1)^2} dA \quad n = 0 \quad (\text{A-28})$$

Hence for $n \geq 1$, we have the recurrence formula

$$G_n(\rho) = 2\rho [n G_{n-2}(\rho) - G_{n-1}(\rho)] \quad (\text{A-29})$$

We denote the integral in (A-28) for $n = 0$ by $2\rho G_{-1}(\rho)$

$$2\rho G_{-1}(\rho) = 2\rho \int_0^{\infty} e^{-\rho(A+1)^2} dA \quad (\text{A-30})$$

$$= \int_{+1}^{\infty} e^{-\rho\xi^2} 2\rho d\xi$$

$$= \int_0^{\infty} e^{-\rho\xi^2} 2\rho d\xi - \int_0^1 e^{-\rho\xi^2} 2\rho d\xi$$

$$2\rho G_{-1}(\rho) = \sqrt{\pi\rho} (1 - \text{erf}(\sqrt{\rho})) \quad (\text{A-31})$$

where $\text{erf } x$ is defined by

$$\text{erf } x = \frac{2}{\sqrt{\pi}} \int_0^x e^{-y^2} dy \quad (\text{A-32})$$

$G_0(\rho)$ is therefore

$$G_0(\rho) = e^{-\rho} - \sqrt{\pi\rho} (1 - \text{erf}(\sqrt{\rho})) \quad (\text{A-33})$$

With the following definitions

$$\alpha_0(\rho) = 1 - G_0(\rho) - G_1(\rho) \quad (\text{A-34})$$

$$\alpha_1(\rho) = G_1(\rho) \quad (\text{A-35})$$

$$\alpha_n(\rho) = \frac{1}{n!} G_n(\rho) \quad n \geq 2 \quad (\text{A-36})$$

we may write

$$m_1(\beta, \rho) = \alpha_0(\rho)\beta + \alpha_1(\rho)\sin\beta - \sum_{n=2}^{\infty} \alpha_n(\rho) I_n(\beta) \quad (\text{A-37})$$

With $\beta = \beta_s \sin \omega_m t$, the amplitude of the fundamental harmonic of $m_1(\beta_s \sin \omega_m t, \rho)$, $A_1(\beta_s, \rho)$ is

$$A_1(\beta_s, \rho) = \alpha_0(\rho) \beta_s + \alpha_1(\rho) 2 J_1(\beta_s) - \sum_{n=2}^{\infty} \alpha_n(\rho) F_n(\beta_s) \quad (\text{A-38})$$

where

$$F_n(\beta_s) = \sum_{k=0}^n \frac{1}{2^{n-1}} b_{n,k} \left(\frac{2}{k} J_1(k\beta_s) \right) \quad (\text{A-39})$$

The signal power out, $S_o(\beta_s, \rho)$, is therefore

$$\begin{aligned} S_o(\beta_s, \rho) &= \frac{1}{2} A_1^2(\beta_s, \rho) \\ &= \frac{1}{2} \left(\alpha_0(\rho) \beta_s + \alpha_1(\rho) 2 J_1(\beta_s) \right)^2 - \epsilon(\beta_s, \rho) \end{aligned} \quad (\text{A-40})$$

where

$$\begin{aligned} \epsilon(\beta_s, \rho) &= \left(\alpha_0(\rho) \beta_s + \alpha_1(\rho) 2 J_1(\beta_s) \right) \sum_{n=2}^{\infty} \alpha_n(\rho) F_n(\beta_s) \\ &\quad - \frac{1}{2} \left(\sum_{n=2}^{\infty} \alpha_n(\rho) F_n(\beta_s) \right)^2 \end{aligned} \quad (\text{A-41})$$

The signal power out is broken up into these two parts since $\epsilon(\beta_s, \rho)$ is much smaller than the first term in (A-40) if β_s is not too large (less than about 2 radians), and $\epsilon(\beta_s, \rho)$ becomes completely negligible compared to the first term in (A-40) as $\rho \rightarrow \infty$ and $\rho \rightarrow 0$. This behavior is illustrated in Fig. 7 where $\frac{1}{2} \left(\alpha_0(\rho) \beta_s + \alpha_1(\rho) 2 J_1(\beta_s) \right)^2$ and $\epsilon(\beta_s, \rho)$ are plotted as a function of ρ for $\beta_s = 0.5, 1.0, 1.5,$ and 2.0 radians.

We now show that as $\rho \rightarrow \infty$, $S_o(\beta_s, \rho)$ approaches $\frac{1}{2} \beta_s^2$ ($\beta_s < \pi$), and that as $\rho \rightarrow 0$, $S_o(\beta_s, \rho)$ approaches $2(\pi\rho) J_1^2(\beta_s)$. To do this we make use of the asymptotic forms of $2\rho G_{-1}(\rho)$ in the limits $\rho \rightarrow \infty$.

$$2\rho G_{-1}(\rho \rightarrow 0) = \sqrt{\pi\rho} (1 - \operatorname{erf}(\sqrt{\rho})) \rightarrow \sqrt{\pi\rho} - 2\rho \left(1 - \frac{\rho}{3 \cdot 1!} + \frac{\rho^2}{5 \cdot 2!} - \frac{\rho^3}{7 \cdot 3!} + \dots\right) \quad (\text{A-42})$$

$$2\rho G_{-1}(\rho \rightarrow \infty) = \sqrt{\pi\rho} (1 - \operatorname{erf}(\sqrt{\rho})) \rightarrow e^{-\rho} \left(1 - \frac{1}{2\rho} + \frac{1 \cdot 3}{(2\rho)^2} - \frac{1 \cdot 3 \cdot 5}{(2\rho)^3} + \dots\right) \quad (\text{A-43})$$

Hence as $\rho \rightarrow \infty$

$$G_0(\rho) = e^{-\rho} - 2\rho G_{-1}(\rho) \rightarrow \frac{1}{2\rho} e^{-\rho} \left(1 - \frac{1 \cdot 3}{2\rho} + \frac{1 \cdot 3 \cdot 5}{(2\rho)^2} - \dots\right) \quad (\text{A-44})$$

which approaches zero as $\frac{1}{2\rho} e^{-\rho}$. As $\rho \rightarrow 0$

$$G_0(\rho) = e^{-\rho} - 2\rho G_{-1}(\rho) \rightarrow 1 - \rho + \frac{\rho^2}{2!} - \frac{\rho^3}{3!} + \dots \\ - \sqrt{\pi\rho} + 2\rho \left(1 - \frac{\rho}{3 \cdot 1!} + \frac{\rho^2}{5 \cdot 2!} - \dots\right)$$

$$G_0(\rho \rightarrow 0) = 1 - \sqrt{\pi\rho} + \rho - \frac{1}{6} \rho^2 + \frac{1}{30} \rho^3 - \dots \quad (\text{A-45})$$

For $n \geq 1$ the recurrence formula (A-29) is used in conjunction with (A-42) to A-45) to obtain the asymptotic behavior of $G_n(\rho)$, and hence of $\alpha_n(\rho)$. For example, for $n = 1$, the asymptotic behavior of $G_1(\rho)$ as $\rho \rightarrow 0$ and $\rho \rightarrow \infty$ is

$$G_1(\rho) = 2\rho G_{-1}(\rho) - 2\rho G_0(\rho)$$

$$G_1(\rho \rightarrow 0) \rightarrow \sqrt{\pi\rho} - 2\rho \left(1 - \frac{\rho}{3 \cdot 1!} + \frac{\rho^2}{5 \cdot 2!} - \dots\right) \\ - 2\rho \left[1 - \sqrt{\pi\rho} + \rho - \frac{1}{6} \rho^2 + \dots\right]$$

$$G_1(\rho \rightarrow 0) = \sqrt{\pi\rho} - 4\rho + 2\rho\sqrt{\pi\rho} - \frac{4}{3} \rho^2 + \dots \quad (\text{A-46})$$

and

$$G_1(\rho \rightarrow \infty) \rightarrow e^{-\rho} \left(1 - \frac{1}{2\rho} + \frac{1 \cdot 3}{(2\rho)^2} - \frac{1 \cdot 3 \cdot 5}{(2\rho)^3} + \dots \right)$$

$$- e^{-\rho} \left(1 - \frac{1 \cdot 3}{2\rho} + \frac{1 \cdot 3 \cdot 5}{(2\rho)^2} - \frac{1 \cdot 3 \cdot 5 \cdot 7}{(2\rho)^3} + \dots \right)$$

$$G_1(\rho \rightarrow \infty) = \frac{1}{\rho} e^{-\rho} \left(1 - \frac{1 \cdot 3 \cdot 2}{2\rho} + \frac{1 \cdot 3 \cdot 5 \cdot 3}{(2\rho)^2} - \frac{1 \cdot 3 \cdot 5 \cdot 7 \cdot 4}{(2\rho)^3} + \dots \right) \quad (\text{A-47})$$

Hence the asymptotic behavior of $\alpha_0(\rho)$, considering the first two leading terms only, is

$$\alpha_0(\rho) = 1 - G_0(\rho) - G_1(\rho)$$

$$\alpha_0(\rho \rightarrow \infty) \rightarrow 1 - \frac{3}{2\rho} e^{-\rho} \quad (\text{A-48})$$

$$\alpha_0(\rho \rightarrow 0) \rightarrow 3\rho - 2\rho\sqrt{\pi\rho} \quad (\text{A-49})$$

The asymptotic behavior of $\alpha_1(\rho)$ is

$$\alpha_1(\rho) = G_1(\rho)$$

$$\alpha_1(\rho \rightarrow \infty) \rightarrow \frac{1}{\rho} e^{-\rho} \left(1 - \frac{3}{\rho} + \dots \right) \quad (\text{A-50})$$

$$\alpha_1(\rho \rightarrow 0) \rightarrow \sqrt{\pi\rho} - 4\rho \quad (\text{A-51})$$

The dominant terms in the asymptotic behavior of $\alpha_n(\rho)$ as $\rho \rightarrow 0$ and $\rho \rightarrow \infty$ for $n = 0, 1, 2, 3, 4, 5, 6, 7$, and 8 are listed in Table A-2. The situation for $n \geq 9$ may readily be deduced from Table A-2.

Hence $\alpha_1(\rho)$ dominates as $\rho \rightarrow 0$, and $\alpha_0(\rho)$ dominates as $\rho \rightarrow \infty$. Consequently,

$$S_0(\beta_s, \rho \rightarrow 0) \rightarrow 2\alpha_1^2(\rho) J_1^2(\beta_s) \rightarrow 2\pi\rho J_1^2(\beta_s) \quad (\text{A-52})$$

and

$$S_0(\beta_s, \rho \rightarrow \infty) \rightarrow \frac{1}{2} \alpha_0^2(\rho) \beta_s^2 \rightarrow \frac{1}{2} \beta_s^2 \quad (\text{A-53})$$

Table A-2

Asymptotic Behavior of $\alpha_n(\rho)$

\underline{n}	$\frac{\alpha_n(\rho \rightarrow 0)}{n}$	$\frac{\alpha_n(\rho \rightarrow \infty)}{n}$
0	3ρ	1
1	$\sqrt{\pi\rho}$	$2 e^{-\rho}/2\rho$
2	(2ρ)	$3 e^{-\rho}/2\rho$
3	$\frac{1}{2} (2\rho) \sqrt{\pi\rho}$	$4 e^{-\rho}/2\rho$
4	$\frac{1}{3} (2\rho)^2$	$5 e^{-\rho}/2\rho$
5	$\frac{1}{2} \cdot \frac{1}{4} (2\rho)^2 \sqrt{\pi\rho}$	$6 e^{-\rho}/2\rho$
6	$\frac{1}{3} \cdot \frac{1}{5} (2\rho)^3$	$7 e^{-\rho}/2\rho$
7	$\frac{1}{2} \cdot \frac{1}{4} \cdot \frac{1}{6} (2\rho)^3 \sqrt{\pi\rho}$	$8 e^{-\rho}/2\rho$
8	$\frac{1}{3} \cdot \frac{1}{5} \cdot \frac{1}{7} (2\rho)^4$	$9 e^{-\rho}/2\rho$

APPENDIX B

Calculation of N_o for the Cross-Over Detector

The second moment $m_2(\beta, \rho)$ for the cross-over detector is

$$m_2(\beta, \rho) = \int_{-\pi}^{\pi} T^2 (\beta + \theta_n) q(\theta_n) d\theta_n \quad (B-1)$$

which, for $\beta > 0$, is

$$\begin{aligned} m_2(\beta, \rho) &= \int_{-\pi}^{\pi} (\beta + \theta_n)^2 q(\theta_n) d\theta_n \\ &+ 4\pi^2 \int_{\pi-\beta}^{\pi} \left[1 - \frac{1}{\pi}(\beta + \theta_n)\right] q(\theta_n) d\theta_n \end{aligned} \quad (B-2)$$

$$= \sigma_{\theta_n}^2(\rho) + \beta^2 + 4\pi^2 \int_{\pi-\beta}^{\pi} \left[1 - \frac{1}{\pi}(\beta + \theta_n)\right] q(\theta_n) d\theta_n \quad (B-3)$$

where $\sigma_{\theta_n}^2(\rho)$ is given by

$$\sigma_{\theta_n}^2(\rho) = \int_{-\pi}^{\pi} \theta_n^2 q(\theta_n) d\theta_n \quad (B-4)$$

and is the noise power that would be measured with the modulation turned off. This has been computed by Chadima¹ and is plotted in Fig. 14. To evaluate the last integral in (B-3) we again introduce the variable $\phi = \pi - \theta_n$ so that $m_2(\beta, \rho)$ becomes

$$m_2(\beta, \rho) = \sigma_{\theta_n}^2(\rho) + \beta^2 + 4\pi \int_0^{\beta} (\phi - \beta) q(\pi - \phi) d\phi \quad (B-5)$$

With $q(\theta_n)$ as given in (A-4) and (A-5), $m_2(\beta, \rho)$ becomes

$$m_2(\beta, \rho) = \sigma_{\theta_n}^2(\rho) + \beta^2 + 2 \int_0^\infty (2\rho A) e^{-\rho(A+1)^2} dA \int_0^\beta (\phi - \beta) e^{2\rho A(1 - \cos \phi)} d\phi \quad (B-6)$$

Expressing $e^{2\rho A(1 - \cos \phi)}$ as in (A-8) and making use of Eq. (A-15), and the definition of $G_n(\rho)$ from (A-11), $m_2(\beta, \rho)$ becomes

$$\begin{aligned} m_2(\beta, \rho) = & \sigma_{\theta_n}^2(\rho) + \beta^2 + 2 G_0(\rho) \int_0^\beta (\phi - \beta) d\phi \\ & + 2 G_1(\rho) \int_0^\beta (\phi - \beta) d\phi - 2 G_1(\rho) \int_0^\beta (\phi - \beta) \cos \phi d\phi \\ & + 2 \sum_{n=2}^\infty \frac{1}{n!} G_n(\rho) \sum_{k=0}^n \frac{b_{n,k}}{2^{n-1}} \int_0^\beta (\phi - \beta) \cos k \phi d\phi \end{aligned} \quad (B-7)$$

Integrating twice by parts we obtain

$$\begin{aligned} \int_0^\beta (\phi - \beta) \cos k \phi d\phi &= -\frac{1}{2} \beta^2 \quad k = 0 \\ &= -\frac{(1 - \cos k\beta)}{k^2} \quad k \geq 1 \end{aligned} \quad (B-8)$$

so that $m_2(\beta, \rho)$ becomes

$$\begin{aligned} m_2(\beta, \rho) = & \sigma_{\theta_n}^2(\rho) + (1 - G_0(\rho) - G_1(\rho)) \beta^2 + G_1(\rho) 2(1 - \cos \beta) \\ & - 2 \sum_{n=2}^\infty \frac{1}{n!} G_n(\rho) H_n(\beta) \end{aligned} \quad (B-9)$$

where

$$H_n(\beta) = \sum_{k=0}^n \frac{b_{n,k}}{2^{n-1}} \left(\frac{1 - \cos k\beta}{k^2} \right) \quad (B-10)$$

or, with $\alpha_n(\rho)$ as defined in (A-34) through (A-36),

$$m_2(\beta, \rho) = \sigma_{\theta_n}^2(\rho) + \alpha_0(\rho) \beta^2 + \alpha_1(\rho) (1 - \cos \beta) - \sum_{n=2}^{\infty} \alpha_n(\rho) H_n(\beta) \quad (\text{B-11})$$

With $\beta = \beta_s \sin \omega_m t$, $\langle m_2(\beta_s \sin \omega_m t, \rho) \rangle_t$ is

$$\begin{aligned} \langle m_2(\beta_s \sin \omega_m t, \rho) \rangle_t &= \sigma_{\theta_n}^2(\rho) + \alpha_0(\rho) \frac{1}{2} \beta_s^2 + \alpha_1(\rho) (1 - J_0(\beta_s)) \\ &\quad - 2 \sum_{n=2}^{\infty} \alpha_n(\rho) E_n(\beta_s) \end{aligned} \quad (\text{B-12})$$

where

$$E_n(\beta_s) = \sum_{k=0}^n \frac{b_{n,k}}{2^{n-1}} \left(\frac{1 - J_0(k\beta_s)}{k^2} \right) \quad (\text{B-13})$$

The noise power out, $N_o(\beta_s, \rho)$ from (23) is

$$\begin{aligned} N_o(\beta_s, \rho) &= \sigma_{\theta_n}^2(\rho) + \alpha_0(\rho) \frac{1}{2} \beta_s^2 + \alpha_1(\rho) (1 - J_0(\beta_s)) \\ &\quad - 2 \sum_{n=2}^{\infty} \alpha_n(\rho) E_n(\beta_s) - S_o(\beta_s, \rho) \end{aligned} \quad (\text{B-14})$$

Introducing $S_o(\beta_s, \rho)$ from (A-40) and (A-41) and regrouping terms, we may write $N_o(\beta_s, \rho)$ as

$$N_o(\beta_s, \rho) = \sigma_{\theta_n}^2(\rho) + \gamma(\beta_s, \rho) \quad (\text{B-15})$$

where $\gamma(\beta_s, \rho)$ contains the dependence on β_s , and becomes negligible compared

to $\sigma_{\theta_n}^2(\rho)$ as $\rho \rightarrow 0$ and $\rho \rightarrow \infty$ as shown in Fig.14 where $\gamma(\beta_s, \rho)$ is plotted as a function of ρ for $\beta_s = 0.5, 1.0, 1.5,$ and 2.0 .

$$\begin{aligned}
 \gamma(\beta_s, \rho) &= \left\{ \alpha_0(\rho) \frac{1}{2} \beta_s^2 + \alpha_1(\rho) (1 - J_0(\beta_s)) \right. \\
 &\quad \left. - \frac{1}{2} (\alpha_0(\rho) \beta_s + \alpha_1(\rho) 2J_1(\beta_s))^2 \right\} \\
 &\quad + \left\{ \sum_{n=2}^{\infty} \alpha_n(\rho) [(\alpha_0(\rho) \beta_s + \alpha_1(\rho) 2J_1(\beta_s)) F_n(\beta_s) - 2E_n(\beta_s)] \right. \\
 &\quad \left. - \frac{1}{2} \left(\sum_{n=2}^{\infty} \alpha_n(\rho) F_n(\beta_s)^2 \right) \right\} \tag{B-16}
 \end{aligned}$$